Multiple mantle metasomatism beneath the Leizhou Peninsula, South China: Evidence from elemental and Sr-Nd-Pb-Hf isotope geochemistry of the late Cenozoic volcanic rocks

Journal:	*International Geology Review*
Manuscript ID	TIGR-2018-0204.R4
Manuscript Type:	Data Article
Date Submitted by the Author:	11-Nov-2018
Complete List of Authors:	Sun, Pu; Institute of Oceanology Chinese Academy of Sciences, Marine geology NIU, Yaoling; Institute of Oceanology, Chinese Academy of Sciences; Durham University Guo, Pengyuan; Institute of Oceanology Chinese Academy of Sciences Chen, Shuo; Institute of Oceanology Chinese Academy of Sciences Duan, Meng ; Institute of Oceanology Chinese Academy of Sciences Gong, Hongmei; Institute of Oceanology, Chinese Academy of Sciences Wang, Xiaohong; Institute of Oceanology Chinese Academy of Sciences Xiao, Yuanyuan; Institute of Oceanology Chinese Academy of Sciences
Keywords:	South China, Cenozoic volcanism, mantle metasomatism, low-F melt, recycled UCC material

1. These rocks show incompatible element enrichment but variable isotopic depletion;
2. High bulk-rock Sr does not indicate recycled oceanic gabbro in the mantle source;
3. A low-F melt with high Sr enriched the incompatible elements of the mantle source;
4. A recently recycled UCC material is present in the mantle source region.

Multiple mantle metasomatism beneath the Leizhou Peninsula, South China: Evidence from elemental and Sr-Nd-Pb-Hf isotope geochemistry of the late Cenozoic volcanic rocks

Pu Sun [1, 2, 3 *], Yaoling Niu [1, 2, 3, 4, 5 **], Pengyuan Guo [1, 2, 3], Shuo Chen[1, 2, 3], Meng Duan [1, 2, 3], Hongmei Gong [1, 2, 3], Xiaohong Wang [1, 2, 3], Yuanyuan Xiao [1, 2, 3]

[1] Institute of Oceanology, Chinese Academy of Sciences, Qingdao 266071, China

[2] Laboratory for Marine Geology, Qingdao National Laboratory for Marine Science and Technology, Qingdao 266061, China

[3] Center for Ocean Mega-Science, Chinese Academy of Sciences, 7 Nanhai Road, Qingdao, 266071, China

[4] Department of Earth Sciences, Durham University, Durham DH1 3LE, UK

[5] School of Earth Science and Resources, China University of Geosciences, Beijing 100083, China

Correspondence:

* Mr. Pu Sun (pu.sun@foxmail.com)

** Professor Yaoling Niu (yaoling.niu@durham.ac.uk)

Abstract. We analyzed whole-rock major and trace elements and Sr-Nd-Pb-Hf isotopes of the late Cenozoic volcanic rocks in the Leizhou Peninsula, South China to investigate their mantle source characteristics. These volcanic rocks, collected from Jiujiang, Tianyang and Huoju areas of the Leizhou Peninsula, are characterized by incompatible element enrichment but variable isotopic depletion. The volcanic rocks from Jiujiang and Tianyang show prominent primitive-mantle-normalized positive Nb, Ta and Sr anomalies and depleted Sr-Nd-Pb-Hf isotope compositions, whereas those from Huoju

show slight positive to negative Nb and Ta anomalies, a prominent positive Pb anomaly, and more enriched Sr-Nd-Pb-Hf isotope compositions. Two types of mantle metasomatism are required to explain the geochemical characteristics of these rocks. The Jiujiang and Tianyang samples were largely derived from a mantle source metasomatized recently by a low-F melt. Such low-F melt is generated within the asthenospheric mantle, which is enriched in volatiles and incompatible elements with positive Sr anomaly and depleted Sr-Nd-Pb-Hf isotope compositions. The Huoju samples were largely derived from a mantle source metasomatized by recycled upper continental crust (UCC) material. These two types of mantle metasomatism beneath the Leizhou Peninsula are consistent with trace element characteristics of mantle mineralogy (e.g., clinopyroxene vs. amphibole), which reflects source evolution in space and time (e.g., tectonic setting change).

Key words: South China; Cenozoic volcanism; mantle metasomatism; low-F melt; recycled UCC material

1. Introduction

Studies of oceanic basalts have revealed mantle chemical heterogeneity on all scales. Although the origin of mantle heterogeneity is controversial, seafloor subduction has long been inferred to be significant in causing the heterogeneity (e.g., Hofmann and White, 1982; Zinder and Hart, 1986; Hart, 1988; Farley, 1995; Stracke et al., 2003; Willbold and Stracke, 2006). Seafloor subduction can carry terrigenous and pelagic sedimentary materials into the upper mantle, which has been inferred to be significant in forming geochemically enriched mantle sources (e.g., Weaver, 1991;

Chauvel et al., 1992; Farley, 1995; Jackson et al., 2007). On the other hand, a low degree (low-F) melt derived within the seismic low velocity zone (LVZ) beneath oceanic lithosphere, which is highly enriched in volatiles, alkalis and incompatible elements, has been suggested to metasomatize the mantle source of intraplate volcanic rocks (Hanson, 1977; Wood, 1979; Halliday et al., 1995; Niu et al., 1999, 2002, 2012; Niu and O'Hara, 2003; Niu, 2005, 2008, 2014; Pilet et al., 2008). The presence of LVZ has also been observed beneath continental lithosphere of eastern Asia, eastern Australia and western America through seismic tomography (Ekström and Dziewonski, 1998), which has been thought to be significant in forming geochemically enriched continental intraplate basalts (e.g., Niu, 2005, 2014; Guo et al., 2016; Sun et al., 2017).

Late Cenozoic intraplate volcanic rocks are widespread in Southeast Asia (Fig. 1a), including those in the South China Sea Basin (Yan et al., 2006; Yan et al., 2015), in the Indochina Peninsula (Hoang and Flower, 1998), and in the Hainan Island and Leizhou Peninsula (Tu et al., 1991, 1992; Flower et al., 1992; Zhang et al., 1996; Ho et al., 2000; Xu et al., 2002; Zou and Fan, 2010; Wang et al., 2011, 2013; Liu et al., 2015). They are characterized by OIB (oceanic island basalts)-like incompatible element enrichment but varying extent of Sr-Nd isotope depletion with a Dupal-type Pb isotope signature (Tu et al., 1991, 1992; Flower et al., 1992; Hoang and Flower, 1998; Chen et al., 2009; Zeng et al., 2013). Over the last decade, a mantle plume has been popularly invoked to explain the petrogenesis of these volcanic rocks, largely inferred from a mantle seismic tomography beneath the region (Lebedev and Nolet, 2003; Zhao, 2004; Yan and Shi, 2007; Lei et al., 2009; Wang et al., 2011) although this interpretation remains debatable.

In this paper, we do not intend to discuss the plume debate, but focus on the mantle source heterogeneity of mantle metasomatic origin using bulk-rock major and trace elements and Sr-Nd-Pb-Hf isotopes of the late Cenozoic volcanic rocks from the

Leizhou Peninsula. These rocks have been relatively poorly studied compared with other Cenozoic volcanic rocks in the Southeast Asia (Ho et al., 2000), which may provide new perspectives on the mantle source characteristics and mantle evolution histories beneath this area. We have identified two types of mantle metasomatism beneath this region: metasomatism genetically derived from melting of subducted terrigenous sediments (upper continental crust material), and the metasomatism by an incompatible element enriched low-F melt derived from the asthenosphere.

2. Geological setting and samples

The Leizhou Peninsula is located at the geological transition between South China continental margin and the South China Sea Basin (SCSB; Fig. 1a). Southeast Asia is geologically considered as an assembly of exotic continental terranes fragmented from Gondwana with the amalgamation largely completed during the early Mesozoic (Lin et al., 1985; Metcalfe, 1990; Tu et al., 1991; Chung et al., 1994; Zou et al., 2000). South China in the Mesozoic was characterized by having an active continental margin with extensive subduction-related granitoid magmatism (Jahn et al., 1990; Zhou and Li, 2000; Li et al., 2012; Niu et al., 2015). The subduction was predicted to cease at ~ 100 Ma because of trench jam by an exotic micro-continent (Niu et al., 2015). The South China Sea is thought to open at ~ 32 Ma and spread until ~ 15.5 Ma (Taylor and Hayes, 1983; Briais et al., 1993; Kido et al., 2001). The intraplate magmatism on the periphery of the SCSB contemporaneous with the SCSB spreading was limited, but resumed extensively after the cessation of the SCSB spreading (Yan et al., 2006; Huang et al., 2013).

The Ar-Ar and K-Ar dating gives erupting ages of 6.12 to 0.17 Ma for the volcanic

rocks in the Leizhou Peninsula (Ho et al., 2000). Our samples were collected from Huoju, Jiujiang and Tianyang areas (Fig. 1b). These volcanic lavas show layered structures (Fig. 2a), caused by multiple episodes of eruptions (Ho et al., 2000). Porous and ropy structures can be observed at the surface of each lava layer (Fig. 2b). These rocks show intergranular texture, with phenocrysts and microlites of olivine, clinopyroxene and magnetite aggregated between euhedral plagioclase laths (~ 0.5-1 mm; Figs. 2c & d). Spinel peridotite mantle xenoliths and clinopyroxene megacrysts are present in volcanic rocks from Jiujiang and Tianyang (Yu et al., 2006; Huang et al., 2007).

3. Sample preparation and analytical procedures

We crushed fresh rocks to chips of ≤ 5 mm before repeatedly cleaned in Milli-Q water in an ultrasonic bath, dried and grounded into ≥ 200 μm powders with an agate mill in a clean environment. Bulk-rock major elements were analyzed at China University of Geosciences, Beijing (CUGB), using a Leeman Prodigy Inductively Coupled Plasma Optical Emission Spectrometer (ICP-OES). Repeated analyses of USGS reference rock standards RCR-1, AGV-2 and national geological standard reference materials GSR-3 give analytical precision better than 1% for most elements except for TiO_2 (~ 1.5%) and P_2O_5 (~ 2.0%). The analytical details are given in Song et al. (2010). See Supplementary Table 1 for major element analytical results for USGS standard AGV-2.

Bulk-rock trace elements were analyzed in the Institute of Oceanology, Chinese Academy of Sciences (IOCAS), using Agilent-7900 inductively coupled plasma mass spectrometer (ICP-MS). Fifty milligrams of each sample were dissolved with acid mix

of distilled HCl+3HNO_3 and HF in a high-pressure jacket equipped Teflon beaker for 15 hours, and then re-dissolved with 20% HNO_3 for 2 hours till complete digestion. Repeated analyses of USGS reference rock standards AGV-2, W-2, BHVO-2, BCR-2 give analytical precisions better than 5% for most elements. See Chen et al. (2017) for analytical details. See Supplementary Table 1 for trace element analytical results for USGS standard AGV-2.

Bulk-rock Sr-Nd-Pb-Hf isotope ratios were measured using a Nu Plasma MC-ICP-MS in the IOCAS. About 50 mg of rock powder was dissolved with double distilled HNO_3 + HCl + HF in a high-pressure jacket equipped Teflon beaker at 190°C for 15 hours, which was then dried and re-dissolved with 2 ml 3N HNO_3 for 2h. The final sample solution was first loaded onto Sr-spec resin columns to separate Sr and Pb, with the eluted sample solution collected and then loaded onto AG 50W-X8 resin columns to separate REE. The eluted sample solution from AG 50W-X8 resin columns was collected and then loaded onto Ln-spec resin columns to collect Hf. The separated REE solution was dried and re-dissolved with 0.25 N HCl before being loaded onto Ln-spec resin columns to collect Nd. The above streamlined procedure was modified after Pin et al. (2014) and Yang et al. (2010). The measured $^{87}Sr/^{86}Sr$, $^{143}Nd/^{144}Nd$ and $^{176}Hf/^{177}Hf$ isotope ratios were normalized for instrumental mass fraction using the exponential law to $^{86}Sr/^{88}Sr = 0.1194$, $^{146}Nd/^{144}Nd = 0.7219$ and $^{179}Hf/^{177}Hf = 0.7325$, respectively. International standards of NBS-987, JNdi-1 and Alfa Hf were used as bracketing standards every five samples to monitor the instrument drift during the analysis of Sr, Nd and Hf isotopes, respectively. Repeated analysis for NBS-987 gives an average $^{87}Sr/^{86}Sr = 0.710245 \pm 0.000012$ (n = 11, 2σ). Repeated analysis for JNdi-1 gives an average $^{143}Nd/^{144}Nd = 0.512094 \pm 0.000008$ (n = 13, 2σ), and repeated analysis for Alfa Hf gives an average $^{176}Hf/^{177}Hf = 0.282194 \pm 0.000007$ (n = 7, 2σ). Pb isotope ratios

were normalized for instrumental mass fraction relative to NBS/SRM 997 $^{203}Tl/^{205}Tl$ = 0.41891. The international standard NBS-981 was used to monitor the instrument drift during the analysis of Pb isotopes. Repeated analysis of NBS-981 gives average $^{206}Pb/^{204}Pb$ = 16.932 ± 0.001 (n = 10, 2σ), $^{207}Pb/^{204}Pb$ = 15.489 ± 0.003 (n = 10, 2σ), and $^{208}Pb/^{204}Pb$ = 36.684 ± 0.013 (n = 10, 2σ). See Supplementary Table 2 for the Sr-Nd-Pb-Hf isotopic results of USGS standards of BCR-2 and AGV-2.

4. Geochemistry

4.1 Major element compositions

The analytical data are given in Supplementary Table 1. For comparison, we also compiled major elements, trace elements and Sr-Nd-Pb isotope data of the Cenozoic basaltic rocks in the Hainan Island (Supplementary Table 3; Tu et al., 1991; Flower et al., 1992; Zou and Fan, 2010; Ho et al., 2000; Wang et al., 2011). The volcanic rocks from the Leizhou Peninsula are mainly tholeiitic and show basaltic-andesitic SiO_2 contents of 47.78-61.21 wt.% with $Mg^{\#}$ of 53-65 (Fig. 3a). The samples from Huoju have highly evolved SiO_2 contents of 54.87-61.21wt.%. The volcanic rocks from the Leizhou Peninsula have comparable Na_2O and K_2O contents with the basaltic rocks from the Hainan Island (Figs. 3b & c). Samples from Jiujiang and Tianyang show apparent higher Al_2O_3 than those from Huoju and Hainan Island (Fig. 3d).

4.2 Trace element compositions

Trace element data are given in Supplementary Table 1. These volcanic rocks

show varying extents of light rare earth element (LREE) enrichment, with OIB-like $[La/Yb]_N$ (chondrite normalized) of 6.0-12.9. They show REE abundances relatively less enriched than OIB, with slight positive Eu anomaly. One sample from Tianyang (ZC11-02) with negative Ce (Fig. 4a), Zr and Hf anomalies (Fig. 4b) and very high Ba/Zr (1.97) and Lu/Hf (0.11) ratios is best explained to reflect significant zircon crystallization because Ce^{4+} substitute Zr and Hf in zircon (Trail et al., 2012).

In the primitive-mantle normalized multi-element spider diagram (Fig. 4b), these volcanic rocks are enriched in incompatible elements, and tend to be more enriched in more incompatible elements, except for Nb, Ta, Pb and Sr, which are anomalous. The Huoju samples show varying Nb and Ta anomalies (from slight positive to negative), moderate positive Sr anomaly and prominent positive Pb anomaly. The samples from Jiujiang and Tianyang have positive Nb and Ta anomalies, weak to moderate positive Pb anomaly and significant positive Sr anomaly. The differences in Nb, Ta, Sr and Eu anomalies of these volcanic rocks are more apparent in Fig. 5, with the ratios of $[Nb/Th]_N$ and $[Ta/U]_N$ falling between those of OIB and upper continental crust (UCC), and Sr/Sr^* and Eu/Eu^* higher than average OIB and most rocks from the Hainan Island. Furthermore, the samples from Huoju have lower $[Nb/Th]_N$, $[Ta/U]_N$, Sr/Sr^* and Eu/Eu^* compared with those from Jiujiang and Tianyang.

4.3 Sr-Nd-Pb-Hf isotopes

The Sr, Nd, Pb and Hf isotope data are given in Supplementary Table 2 and shown in Fig. 6. In general, these rocks have more variable Sr-Nd-Pb isotopic compositions than rocks from the Hainan Island, and plot in the field of the Cenozoic basalts from SCSB (Figs. 6a, c & d). They have generally depleted $^{87}Sr/^{86}Sr$ (0.702955-0.704888),

$^{143}Nd/^{144}Nd$ (0.512754-0.512998) and $^{176}Hf/^{177}Hf$ (0.282939-0.283124), with ε_{Nd} of +2.3 to +7.0 and ε_{Hf} of +5.5 to +12.0, respectively. However, they have radiogenic $^{207}Pb/^{204}Pb$ (15.530-15.666) and $^{208}Pb/^{204}Pb$ (38.425-39.077) with intermediate $^{206}Pb/^{204}Pb$ (18.454-18.727).

These rocks in Sr-Nd isotopic space define a negative trend (Fig. 6a), which extends from the field of the depleted mid-ocean ridge basalts (MORB) to the more enriched OIB field. The positive Nd-Hf isotopic correlation is subparallel to the terrestrial array (Vervoort et al., 1999; Fig. 6b). A high-angle trend away from the Northern Hemisphere Reference Line (NHRL; Hart, 1984) in the $^{207}Pb/^{204}Pb$ vs. $^{206}Pb/^{204}Pb$ diagram is significant (Fig. 6c). In the $^{208}Pb/^{204}Pb$ vs. $^{206}Pb/^{204}Pb$ diagram, they plot above and subparallel to the NHRL (Fig. 6d), showing a Dupal signature (Hart, 1984). Besides, there are a positive correlation between $^{206}Pb/^{204}Pb$ and $^{87}Sr/^{86}Sr$ and a negative correlation between $^{206}Pb/^{204}Pb$ and $^{143}Nd/^{144}Nd$ (Figs. 6e & f).

The correlations of Sr-Nd-Pb-Hf isotope ratios of the volcanic rocks from the Leizhou Peninsula are to a first order consistent with two component-mixing in the mantle source region: an Indian-type depleted mantle component and an isotopically enriched component. Compared with samples from Jiujiang and Tianyang, the Huoju samples have higher $^{87}Sr/^{86}Sr$ and $^{206}Pb/^{204}Pb$ and lower $^{143}Nd/^{144}Nd$ and $^{176}Hf/^{177}Hf$ (Fig. 6), indicating higher contribution of the isotopically enriched component in the mantle source region.

5. Discussion

5.1 Effect of fractional crystallization and crustal contamination on magma compositions

Compared with the samples from Jiujiang and Tianyang and the rocks from the Hainan Island, the samples from Huoju show relatively lower $Mg^{\#}$, CaO (Fig. 3e), Ni (Fig. 3g) and Cr (Fig. 3h), reflecting their experiencing higher extent of fractional crystallization. The rocks from the Leizhou Peninsula show generally lower CaO/Al_2O_3 relative to the rocks from the Hainan Island, indicating their experiencing higher extent of crystallization of clinopyroxenes (Cpx; Fig. 3f). According to the correlations of $Mg^{\#}$ with Cr and Ni, these samples must have experienced olivine and Cpx-dominated fractional crystallization (Figs. 3g & h).

Before using bulk-rock trace elements and Sr-Nd-Pb-Hf isotopes to infer source compositional characteristics, we need to evaluate the potential contribution of crustal contamination in the bulk-rock compositions of these volcanic rocks during their ascent to the surface. The continental crust materials are characterized by enriched SiO_2, radiogenic Sr isotopes and unradiogenic Nd isotopes. Therefore, involvement of the continental crust materials in the basaltic melt can increase both SiO_2 and $^{87}Sr/^{86}Sr$ values, while decrease $^{143}Nd/^{144}Nd$ values of the melt. Compared with the samples from Jiujiang and Tianyang, the samples from Huoju show generally higher SiO_2 (54.87-61.21 wt.%) and $^{87}Sr/^{86}Sr$ (0.703882-0.704888) (Fig 7). However, the higher SiO_2 and $^{87}Sr/^{86}Sr$ features of the Huoju samples should not be caused by crustal contamination, and their isotopic compositions were largely inherited from the source materials for the following reasons:

(1) simple mixing calculation shows that to generate the Huoju samples with 54.87-61.21 wt.% SiO_2, as high as ~38-70% UCC materials are needed to assimilate with the assumed "primary" basaltic melt. Even if such high extent of crustal assimilation was possible, it would generate melts with high $^{87}Sr/^{86}Sr$ values of ~0.7071-0.7116 (Fig. 7), much higher than the $^{87}Sr/^{86}Sr$

values (0.703882-0.704888) of the Huoju samples;

(2) there are no co-variations between SiO_2 and $^{87}Sr/^{86}Sr$ values in the Huoju samples (Fig. 7), indicating that the SiO_2 and $^{87}Sr/^{86}Sr$ variations in the Huoju samples were controlled by different processes, rather than one common process of crustal contamination. The higher SiO_2 contents were caused by high extent of fractional crystallization, while the higher $^{87}Sr/^{86}Sr$ values were most likely inherited from the mantle source compositions;

(3) The Sr-Nd-Pb isotope compositions of the volcanic rocks in the Leizhou Peninsula plot in the field of Cenozoic basalts from the SCSB (Fig. 6; Tu et al., 1992; Yan et al., 2008, 2015). These SCSB basalts were erupted through oceanic crust and experienced little continental crust contamination. Hence, the Sr-Nd-Pb isotope compositions of Cenozoic basalts from the SCSB and intraplate volcanic rocks in the periphery regions of the SCSB must reflect mantle signatures, which has been confirmed by studies of the Cenozoic volcanic rocks from Hainan Island (Tu et al., 1991), Vietnam (Hoang et al., 1996; Hoang and Flower, 1998) and Southeast China (Sun et al., 2017, 2018).

5.2 Explanation of the positive Sr anomaly in the volcanic rocks from the Leizhou Peninsula

The volcanic rocks from the Leizhou Peninsula have a significant positive Sr anomaly (Fig. 4b). Such positive Sr anomaly has also been observed in Cenozoic basalts from the Hainan Island (Fig. 8), which was explained to result from the addition of recycled oceanic gabbro in the mantle source region (Wang et al., 2011), because plagioclase-rich oceanic gabbro has high Sr (Sobolev et al., 2000; Yaxley and Sobolev,

2007; Stroncik and Devey, 2011). Hence, the positive Sr anomaly in the Hainan basalts was suggested as evidence for the presence of recycled oceanic crust entrained by an upwelling mantle plume beneath this area (Wang et al., 2011). This explanation is possible and likely. However, this explanation is not suitable for the volcanic rocks in the Leizhou Peninsula, as reflected from the distinct correlation trends of Sr/Sr^* with SiO_2, $[La/Sm]_N$, Nb/U and Zr/Hf between rocks from the Leizhou Peninsula and Hainan Island (Fig. 8). This is because 1) partial melts from recycled gabbroic oceanic crust are characterized by both positive Sr anomaly and more silicic composition (Green and Ringwood, 1968; Wyllie, 1970; Yaxley and Sobolev, 2007). However, the volcanic rocks from the Leizhou Peninsula show negative correlation between SiO_2 and Sr/Sr^* (Fig. 8a); 2) recycled oceanic crust materials are depleted in incompatible elements with low $[La/Sm]_N$ (Niu et al., 2002, 2012; Niu and O'Hara, 2003). However, the volcanic rocks from Jiujiang and Tianyang with higher Sr/Sr^* have higher $[La/Sm]_N$ (primitive mantle normalized) of 2.5-3.3 than the average OIB (~ 2.4; Sun and McDonough, 1989) (Fig. 7b), reflecting an incompatible element enriched mantle source (Niu and Batiza, 1997). Besides, these samples show Nb/U (38.2-61.3) similar to average OIB (47 ± 10; Hofmann et al., 1986) and super chondritic Zr/Hf ratios (38.3-43.3; Dupuy et al., 1992; Niu, 2012) (Figs. 8c & d). As the elements in each ratio pair have similar incompatibility during mantle melting and magma evolution, these ratios thus largely reflect the source ratios (Hofmann et al., 1986; Niu and Batiza, 1997). All the above characteristics suggest that the rocks from the Leizhou Peninsula with a significant positive Sr anomaly (especially those from Jiujiang & Tianyang) are derived from an incompatible element enriched mantle source.

The volcanic rocks from Jiujiang and Tianyang show generally depleted Sr-Nd-Pb-Hf isotope compositions (Fig. 6), indicating their origin from an isotopically

depleted asthenospheric mantle. As inferred from MORB, the asthenospheric mantle is incompatible element depleted, which is thought to result from continental crust extraction in the Earth's early history (Gast, 1968; O'Nions et al., 1979; Allègre et al., 1983). However, as inferred above, the mantle source of the Jiujiang and Tianyang samples is enriched, not depleted, in incompatible elements. Therefore, there must be a process that had re-enriched the incompatible elements in the asthenospheric mantle source of these volcanic rocks. Such process must also account for the significant positive Sr anomaly observed in these samples because of the positive correlations of Sr/Sr^* with $[La/Sm]_N$, Nb/U and Zr/Hf (Fig. 8).

5.3 Low-F melt metasomatism in the mantle source region

Low-degree (low-F) melt metasomatism enriched in volatiles, alkalis and incompatible elements has long been considered significant in forming geochemically enriched mantle source (Halliday et al., 1995; Niu et al., 1996, 2002, 2012; Niu and O'Hara, 2003; Workman et al., 2004; Tang et al., 2006; Niu, 2005, 2008, 2014; Guo et al., 2016; Sun et al., 2017). Such low-F melt may develop within the low velocity zone (LVZ) and is inferred to be more enriched in the more incompatible elements (Niu et al., 1996, 2002, 2012; Niu and O'Hara, 2003). Furthermore, during ascent through the lithosphere, the low-F melt can experience cooling-induced crystallization to form metasomatic amphibolite and/or pyroxenite veinlets (Hanson, 1977; Wood, 1979; Zanetti et al., 1996; Niu, 2008; Pilet et al., 2008). Indeed, the presence of amphiboles, which occurs as interstitial grains in the mantle xenoliths entrained in these volcanic rocks indicates the existence of a modal mantle metasomatism (Yu et al., 2006). Furthermore, these mantle amphiboles are characterized by enriched incompatible

elements and prominent positive Sr anomaly (Fig. 9; $Sr/Sr^* = 1.71\text{-}3.96$) (Yu et al., 2006). Although the partition coefficients of Sr/Sr^* ($D_{Sr/Sr^*} = 2*D_{Sr}/[D_{Pr}+D_{Nd}]$) between amphibole and basaltic melt are experimentally determined to be > 1 ($D_{Sr/Sr^*} = 1.42$, LaTourrette et al., 1995; also see the compilations in Dalpré and Baker (2000)), crystallization of the low-F melt with $Sr/Sr^* = 1$ is still inadequate to form amphiboles with Sr/Sr^* of 1.71-3.96. Therefore, it requires the metasomatic low-F melt having $Sr/Sr^* > 1$ to crystallize the mantle amphiboles with prominent positive Sr anomalies. The volcanic rocks from Jiujiang and Tianyang derived from such low-F melt metasomatized mantle source thus show characteristics of enriched incompatible elements and positive Sr anomalies (Fig. 9).

Because such low-F melt should have high Nd/Sm, U/Pb, Hf/Lu (the element on the numerator is more incompatible than that on the denominator in each ratio pair), it will develop long-time integrated Pb isotopes and unradiogenic Nd and Hf isotopes. However, the samples from Jiujiang and Tianyang with low $^{147}Sm/^{144}Nd$ and $^{176}Lu/^{177}Hf$ and high $^{238}U/^{206}Pb$ have high $^{143}Nd/^{144}Nd$ and $^{176}Hf/^{177}Hf$ and low $^{206}Pb/^{204}Pb$ (Figs. 10b, c, d), which is inconsistent with the characteristics of the low-F melt after long-time decay. Therefore, we support a recent (or "current") low-F melt metasomatism without enough time for isotope intergrowth, which is consistent with the understanding of the mantle metasomatism beneath eastern China (Niu, 2005, 2014; Guo et al., 2016; Sun et al., 2017, 2018). The positive correlation between $^{87}Rb/^{86}Sr$ and $^{87}Sr/^{86}Sr$ (Fig. 10a) gives a pseudochron age of 1298 Ma. As the low-F melt metasomatism has been identified to be recent, this age has no geological significance, but is best explained by melting-induced mixing with the pseudochron slope controlled by the compositions of the two endmembers, i.e., a metasomatic low-F melt with relatively low Rb/Sr and depleted Sr isotope composition and another component with

high Rb/Sr and enriched Sr isotope composition.

5.4 Recycled UCC material metasomatism in the mantle source region

The UCC material is characterized by enrichment in LILEs (large ion lithophile elements) and depletion in HFSEs (high field strength elements; e.g. Nb and Ta) with negative Sr and Eu anomalies, higher Pb/Ce than MORB and OIB and enriched Sr-Pb-Nd-Hf isotopes (Hofmann et al., 1986; Rudnick and Gao, 2003; Jackson et al., 2007; Niu and O'Hara, 2009). Therefore, contribution of the UCC material to the asthenospheric mantle or the mantle-derived melt will decrease the HFSE/LILE ratios (e.g. $[Nb/Th]_N$ and $[Ta/U]_N$), Sr/Sr^*, Eu/Eu^*, $^{143}Nd/^{144}Nd$ and $^{176}Hf/^{177}Hf$, but increase Pb/Ce, $^{87}Sr/^{86}Sr$ and $^{206}Pb/^{204}Pb$ in the melt. The Huoju samples have low $[Nb/Th]_N$, $[Ta/U]_N$, Sr/Sr^* and Eu/Eu^* (Fig. 5) and positive Pb anomaly (Fig. 4) with more enriched Sr-Nd-Pb-Hf isotopes (Fig. 6), which shows apparent crustal signatures. Furthermore, Sr-Pb-Nd-Hf isotope ratios show scattered yet significant correlations with $[Nb/Th]_N$, $[Ta/U]_N$, Sr/Sr^* and Pb/Ce (See Supplementary Figure 1). With Sr-Pb-Nd-Hf isotopes being more enriched, $[Nb/Th]_N$, $[Ta/U]_N$ and Sr/Sr^* decrease while Pb/Ce increasing, which is most consistent with variable extent of incorporation of UCC material in the volcanic rocks in the Leizhou Peninsula.

As we have discussed above, such crustal signatures in these rocks cannot be attributed to the crustal contamination during melt ascent, and thus they must be inherited from the recycled UCC materials in the mantle source region. The UCC material present in the mantle source region was most likely originated from subducted terrigenous sediments. In Figs. 6c & d, the Pb isotope systematics indeed show trends from a CIR (Central Indian Ridge; Mahoney et al., 1989) MORB mantle component to

a Java terrigenous sediment component (Plank and Langmuir, 1998). The above inference confirms our previous interpretations that recycled UCC material must have added to the mantle source region of the Cenozoic basalts in Southeast China (Sun et al., 2017). The Huoju samples with more enriched Sr-Nd-Pb-Hf isotopes, higher Pb/Ce and lower $[Nb/Th]_N$, $[Ta/U]_N$ and Sr/Sr^* must have higher contributions of recycled UCC materials in the mantle source region.

Because clinopyroxene is an important host for incompatible elements in mantle minerals, its elemental and isotopic characteristics have been widely used to study the nature and intensity of the metasomatic event (e.g., Norman, 1998; Xu et al., 2003; Niu, 2004; Zheng et al., 2006; Tang et al., 2008; Wittig et al., 2009, 2010). Studies on the clinopyroxenes in the mantle xenoliths entrained in the Cenozoic volcanic rocks from the Leizhou peninsula show that some clinopyroxenes have high Pb/Ce with relatively low Sr/Sr^*(Fig. 9; Yu et al., 2006), which is consistent with trace element characteristics of the volcanic rocks from Huoju region and Hainan Island and UCC materials. This further substantiates the existence of recycled UCC material in the mantle source region beneath the Leizhou Peninsula and Hainan Island (Tu et al., 1991).

The recycling of UCC material into the asthenospheric mantle must be recent, because 1) ancient (e.g. > 1 Ga) recycled UCC materials with low U/Pb and Th/Pb ratios should have unradiogenic Pb isotope ratios (Stracke et al., 2003), which is in contrast with the radiogenic Pb isotopes of the Huoju samples; 2) The high angle Pb isotope trend away from the NHRL (Fig. 6c) that is often observed in volcanic arc magmas (e.g., Cohen and O'Nions, 1982; Woodhead and Fraster, 1985; Vroon et al., 1993) is more consistent with a recent recycling of UCC material (Hart, 1984; Tu, 1991). Trace element modelling shows that ~ 6-10% UCC materials were mixed in the first place with the depleted MORB mantle (DMM) materials. Such UCC material modified

mantle source was then mixed by variable extents with the metasomatic low-F melt to form the ultimate mantle source of the volcanic rocks in the Leizhou Peninsula (Fig. 11). Subduction of the Pacific plate in the Mesozoic along the present SE China coastline prior to opening of the South China Sea may have contributed this recycled UCC material as terrigenous sediment into the asthenospheric mantle beneath the Leizhou Peninsula (Fig. 12a; Tu et al., 1991). After the opening of the South China Sea, the tectonic setting of the Leizhou Peninsula changed from a subduction zone environment to an intraplate environment. The metasomatic agent in the asthenospheric mantle beneath the Leizhou Peninsula changed from recycled UCC material to a low-F melt derived within the asthenospheric mantle. Such low-F melt is enriched in incompatible elements and volatiles, which is buoyant and tends to ascend to metasomatize the overlying asthenospheric mantle and the base of the lithosphere (Fig. 12b). The above inference may not be exact, but effectively captures the mantle evolution beneath the Leizhou Peninsula in space and time.

6. Conclusion

1) The volcanic rocks in the Leizhou Peninsula show varying elemental and isotopic characteristics. The samples from Jiujiang and Tianyang show significant primitive-mantle-normalized positive Nb, Ta and Sr anomalies with depleted Sr-Nd-Pb-Hf isotope compositions, while some samples from Huoju show significant negative Nb and Ta anomalies, positive Pb anomaly and more enriched Sr-Nd-Pb-Hf isotope compositions.

2) The positive Sr anomaly in the samples from Jiujiang and Tianyang is not evidence for the presence of recycled oceanic gabbro in the mantle source, but is consistent

with the incompatible element enrichment of the mantle source materials.

3) A low-F melt mantle metasomatism which is enriched in volatiles and incompatible elements is required to explain the incompatible element enrichment and positive Sr anomaly in these volcanic rocks. Such mantle metasomatism must take place recently to account for lacking isotope ingrowth in the mantle source regions.

4) Presence of recycled UCC material in the mantle source region is also required to explain the trace element and isotope characteristics of the volcanic rocks from Huoju. These UCC material, in the form of terrigenous sediments, may be subducted recently into the upper mantle.

Acknowledgement

We are grateful to the constructive comments of two anonymous reviewers. This work was supported by the NSFC-Shandong Joint Fund for Marine Science Research Centers (U1606401), the National Natural Science Foundation of China (NSFC Grants 41776067, 41630968, 41130314, 91014003), Chinese Academy of Sciences (Innovation Grant Y42217101L), and grants from Qingdao National Laboratory for Marine Science and Technology (2015ASKJ03) and 111 Project (B18048).

References

Allègre C. J., Hart S. R. and Minster J. F. (1983) Chemical structure and evolution of the mantle and continents determined by inversion of Nd and Sr isotopic data, I. Theoretical methods. *Earth Planet. Sci. Lett.* **66**, 177–190.

Briais A., Patriat P. and Tapponnier P. (1993) Updated interpretation of magnetic

anomalies and seafloor spreading stages in the South China Sea: Implications for the Tertiary tectonics of Southeast Asia. *J. Geophys. Res.* **98**, 6299–6328.

Chauvel C., Hofmann A. W. and Vidal P. (1992) HIMU-EM: the French Polynesian connection. *Earth Planet. Sci. Lett.* **110**, 99-119.

Chen L.-H., Zeng G., Jiang S.-Y., Hofmann A. W., Xu X.-S., and Pan M.-B. (2009) Sources of Anfengshan basalts: Subducted lower crust in the Sulu UHP belt, China: *Earth Planet. Sci. Lett.* **286**, 426-435.

Chen S., Wang X.H., Niu Y.L., Sun P., Duan M., Xiao Y.Y., Guo P.Y., Gong H.M., Wang G.D., Xue Q.Q. (2017) Simple and cost-effective methods for precise analysis of trace element abundances in geological materials with ICP-MS. *Sci. Bull.* **62**, 277-289.

Chung S.-L., Sun S.-s., Tu K., Chen C.-H. and Lee C.-y. (1994) Late Cenozoic basaltic volcanism around the Taiwan Strait, SE China: product of lithosphere-asthenosphere interaction during continental extension. *Chem. Geol.* **112**, 1-20.

Cohen R. and O'Nions R. (1982) Identification of recycled continental material in the mantle from Sr, Nd and Pb isotope investigations. *Earth Planet. Sci. Lett.* **61**, 73-84.

Dalpé C. and Baker D. R. (2000) Experimental investigation of large-ion-lithophile-element, high-field-strength-element and rare-earth-element partitioning between calcic amphibole and basaltic melt: the effects of pressure and oxygen fugacity. *Contrib. Mineral. Petrol.* **140**, 233-250.

Dupuy C., Liotard J. and Dostal J. (1992) Zr/Hf fractionation in intraplate basaltic

rocks: carbonate metasomatism in the mantle source. *Geochim. Cosmochim. Acta* **56**, 2417-2423.

Ekström G. and Dziewonski A. M. (1998) The unique anisotropy of the Pacific upper mantle. *Nature* **394**, 168.

Farley K. (1995) Rapid cycling of subducted sediments into the Samoan mantle plume. *Geology* **23**, 531-534.

Flower M. F., Zhang M., Chen C., Tu K. and Xie G. (1992) Magmatism in the south China basin: 2. Post-spreading Quaternary basalts from Hainan Island, south China. *Chem. Geol.* **97**(1), 65-87.

Gast P. W. (1968) Trace element fractionation and the origin of tholeiitic and alkaline magma types, *Geochim. Cosmochim. Acta* **32**, 1055 – 1086.

Green T. H. and Ringwood A. E. (1968) Genesis of the calc-alkaline igneous rock suite, *Contrib. Mineral. Petrol.* **18**, 105-162.

Guo P., Niu Y., Sun P., Ye L., Liu J., Zhang Y., Feng Y. X. and Zhao J. X. (2016) The origin of Cenozoic basalts from central Inner Mongolia, East China: The consequence of recent mantle metasomatism genetically associated with seismically observed paleo-Pacific slab in the mantle transition zone. *Lithos* **240-243**, 104-118.

Halliday A. N., Lee D.-C., Tommasini S., Davies G. R., Paslick C. R., Fitton J. G. and James D. E. (1995) Incompatible trace elements in OIB and MORB and source enrichment in the sub-oceanic mantle. *Earth Planet. Sci. Lett.* **133**, 379-395.

Hanson G. N. (1977) Geochemical evolution of the suboceanic mantle. *J. Geol. Soc.*

134(2), 235-253.

Hart S. R. (1984) A large-scale isotope anomaly in the Southern Hemisphere mantle. *Nature* **309**, 753-757.

Hart S. R. (1988) Heterogeneous mantle domains: signatures, genesis and mixing chronologies. *Earth Planet. Sci. Lett.* **90**, 273-296.

Ho K., Chen J. and Juang W. (2000) Geochronology and geochemistry of late Cenozoic basalts from the Leiqiong area, southern China. *J. Asian Earth Sci.* **18**(3), 307-324.

Hoang N., Flower M. F. J. and Carlson R. W. (1996) Major, trace element, and isotopic compositions of Vietnamese basalts: Interaction of hydrous EM1-rich asthenosphere with thinned Eurasian lithosphere. *Geochim. Cosmochim. Acta* **60**, 4329-4351.

Hoang N. and Flower M. (1998) Petrogenesis of Cenozoic Basalts from Vietnam: Implication for Origins of a 'Diffuse Igneous Province'. *J. Petrol.* **39**(3), 369-395.

Huang X.-L., Xu Y.-G., Lo C.-H. Wang R.-C. and Lin C.-Y. (2007) Exsolution lamellae in a clinopyroxene megacryst aggregate from Cenozoic basalt, Leizhou Peninsula, South China: petrography and chemical evolution. *Contrib. Mineral. Petrol.* **154**, 691-705.

Huang X.-L., Niu Y., Xu Y.-G., Ma J.-L., Qiu H.-N. and Zhong, J.-W. (2013) Geochronology and geochemistry of Cenozoic basalts from eastern Guangdong, SE China: constraints on the lithosphere evolution beneath the northern margin of the South China Sea. *Contrib. Mineral. Petrol.* **165**, 437-455.

Hofmann A. W. and White W. M. (1982) Mantle plumes from ancient oceanic crust.

Earth Planet. Sci. Lett. **57**, 421-436.

Hofmann A., Jochum K., Seufert M. and White W. (1986) Nb and Pb in oceanic basalts: new constraints on mantle evolution. *Earth Planet. Sci. Lett.* **79**, 33-45.

Jackson M. G., Hart S. R., Koppers A. A. P., Staudigel H., Konter J., Blusztajn J., Kurz M. and Russel J. A. (2007) The return of subducted continental crust in Samoan lavas. *Nature* **448**(7154), 684-687.

Jahn B. M., Zhou X. H. and Li J. L. (1990) Formation and tectonic evolution of southeast China: isotopic and geochemical constraints. *Tectonophysics* **183**, 145-160.

Johnson M. C. and Plank T. (2000) Dehydration and melting experiments constrain the fate of subducted sediments. *Geochem. Geophys. Geosyst*. **1**(12).

Kido Y., Suyehiro K. and Kinoshita H. (2001) Rifting to spreading process along the northern continental margin of the South China Sea. *Marine Geophysical Research* ***22***(1), 1-15.

LaTourrette T., Hervig R. L. and Holloway J. R. (1995) Trace element partitioning between amphibole, phlogopite, and basanite melt. *Earth Planet. Sci. Lett.* **135**, 13-30.

Lebedev S. and Nolet G. (2003) Upper mantle beneath Southeast Asia from S velocity tomography. *J.Geophys. Res.* **108**, 2048.

Lei J., Zhao D., Steinberger B., Wu B., Shen F. and Li Z. (2009) New seismic constraints on the upper mantle structure of the Hainan plume. *Phys. Earth Planet In.* **173**, 33-50.

Li Z. X., Li X. H., Chung S. L., Lo C., Xu X. and Li W. (2012) Magmati switch-on and switch-off along South China continental margin since the Permian: transition from an Andean-type to a western Pacific type. *Tectonophysics* **523–535**, 271–290.

Lin J. L., Fuller M. and Zhang W. Y. (1985) Preliminary Phanerozoic polar wander paths for the North and South China blocks. *Nature* **313**, 444-449.

Liu J. Q., Ren Z-Y., Nichols A., Song M., Qian S., Zhang Y. and Zhao P. (2015) Petrogenesis of Late Cenozoic Basalts from North Hainan Island: Constraints from Melt Inclusions and Their Host Olivines. *Geochim. Cosmochim. Acta*. **152**, 89–121.

Mahoney J., Natland J., White W., Poreda R., Bloomer S., Fisher R. and Baxter A. (1989) Isotopic and geochemical provinces of the western Indian Ocean spreading centers. *J.Geophys. Res.* **94**, 4033-4052.

Metcalfe I. (1990) Allochthonous terrane processes in Southeast Asia. *Philos. Trans. R. Soc. London* **331**, 625-640.

Niu Y. (2004). Bulk-rock major and trace element compositions of abyssal peridotites: implications for mantle melting, melt extraction and post-melting processes beneath mid-ocean ridges. *J. Petrol.* **45**(12), 2423-2458.

Niu Y. (2005) Generation and evolution of basaltic magmas: some basic concepts and a new view on the origin of Mesozoic–Cenozoic basaltic volcanism in eastern China. *Geological Journal of China Universities* **11**, 9-46.

Niu Y. (2008) The origin of alkaline lavas. *Science* **320**, 883-884.

Niu, Y. (2012). Earth processes cause Zr–Hf and Nb–Ta fractionations, but why and how? *RSC Advances* **2**, 3587-3591.

Niu Y. (2014) Geological understanding of plate tectonics: Basic concepts, illustrations, examples and new perspectives. *Global Tectonics and Metallogeny* **10**, 23-46.

Niu Y. and Batiza R. (1997) Trace element evidence from seamounts for recycled oceanic crust in the Eastern Pacific mantle. *Earth Planet. Sci. Lett.* **148**, 471-483.

Niu Y. and O'Hara M. J. (2003) Origin of ocean island basalts: A new perspective from petrology, geochemistry, and mineral physics considerations. *J. Geophys. Res.* **108**, 2209.

Niu Y. and O'Hara M. J. (2009) MORB mantle hosts the missing Eu (Sr, Nb, Ta and Ti) in the continental crust: new perspectives on crustal growth, crust–mantle differentiation and chemical structure of oceanic upper mantle. *Lithos* **112**, 1-17.

Niu Y., Waggoner D. G., Sinton J. M. and Mahoney J. J. (1996) Mantle source heterogeneity and melting processes beneath seafloor spreading centers, the East Pacific Rise, 18–19 S. *J. Geophys. Res.***101**, 27711-27733.

Niu Y., Collerson K. D., Batiza R., Wendt J. I. and Regelous M. (1999) Origin of enriched-type mid-ocean ridge basalt at ridges far from mantle plumes: The East Pacific Rise at 11º 20′ N. *J. Geophys. Res.* **104**(B4), 7067-7087.

Niu Y., Regelous M., Wendt I. J., Batiza R. and O′Hara. (2002) Geochemistry of near-EPR seamounts: importance of source vs. process and the origin of enriched mantle component. *Earth Planet. Sci. Lett.* **199**, 327-345.

Niu Y., Wilson M., Humphreys E. R. and O'Hara M. J. (2012) A trace element perspective on the source of ocean island basalts (OIB) and fate of subducted ocean crust (SOC) and mantle lithosphere (SML). *Episodes* **35**, 310.

Niu Y., Liu Y., Xue Q., Shao F., Chen S., Duan M., Guo P., Gong H., Hu Y., Hu Z., Kong J., Li J., Liu J., Sun P., Sun W., Ye L., Xiao Y. and Zhang Y. (2015) Exotic origin of the Chinese continental shelf: new insights into the tectonic evolution of the western Pacific and eastern China since the Mesozoic. *Sci. Bull.* **60**, 1598-1616.

Norman M. D. (1998) Melting and metasomatism in the continental lithosphere: laser ablation ICPMS analysis of minerals in spinel lherzolites from eastern Australia. *Contrib. Mineral. Petrol.* **130**, 240-255.

O'Nions R. K., Evensen N. M. and Hamilton P. J. (1979) Geochemical modeling of mantle differentiation and crustal growth. *J. Geophys. Res.* **84**, 6091–6101.

Pilet S., Baker M. B. and Stolper E. M. (2008) Metasomatized lithosphere and the origin of alkaline lavas. *Science* **320**, 916-919.

Pin C., Gannoun A. and Dupont A. (2014) Rapid, simultaneous separation of Sr, Pb, and Nd by extraction chromatography prior to isotope ratios determination by TIMS and MC-ICP-MS. *Journal of Analytical Atomic Spectrometry* **29**, 1858-1870.

Plank T. and Langmuir C. H. (1998) The chemical composition of subducting sediment and its consequences for the crust and mantle. *Chem. Geol.* **145**, 325-394.

Rudnick R. L. and Gao S. (2003) Composition of the continental crust. *Treatise on geochemistry* **3**, 1-64.

Salters V.J. and Stracke, A. (2004) Composition of the depleted mantle. *Geochem. Geophys. Geosyst*. **5**.

Sobolev A. V., Hofmann A. W. and Nikogosian I. K. (2000) Recycled oceanic crust observed in 'ghost plagioclase'within the source of Mauna Loa lavas. *Nature* **404**,

986-990.

Song S., Su L., Li X., Zhang G., Niu Y. and Zhang L. (2010) Tracing the 850-Ma continental flood basalts from a piece of subducted continental crust in the North Qaidam UHPM belt, NW China. *Precam. Res.* **183**, 805-816.

Stracke A., Bizimis M. and Salters V. J. (2003) Recycling oceanic crust: quantitative constraints. *Geochem. Geophys. Geosyst*. **4**.

Stroncik N. A. and Devey C. W. (2011) Recycled gabbro signature in hotspot magmas unveiled by plume–ridge interactions. *Nature Geoscience* **4**, 393.

Sun S. and McDonough W. F. (1989) Chemical and isotopic systematics of oceanic basalts: implications for mantle composition and processes. *Geological Society, London, Special Publications* **42**, 313-345.

Sun P., Niu Y., Guo P., Ye L., Liu J. and Feng Y. (2017) Elemental and Sr–Nd–Pb isotope geochemistry of the Cenozoic basalts in Southeast China: Insights into their mantle sources and melting processes. *Lithos* **272–273**, 16-30.

Sun P., Niu Y., Guo P., Cui H., Ye L. and Liu J. (2018) The evolution and ascent paths of mantle xenolith-bearing magma. Observations and insights from Cenozoic basalts in Southeast China. *Lithos* **310–311**, 171-181.

Tang Y.J., Zhang H.F. and Ying J.F. (2006) Asthenosphere-lithospheric mantle interaction in an extensional regime: Implication from the geochemistry of Cenozoic basalts from Taihang Mountains, North China Craton. *Chem. Geol.* **233**, 309-327.

Tang Y.J., Zhang H.F., Ying J.F., Zhang J. and Liu X.M. (2008) Refertilization of

ancient lithospheric mantle beneath the central North China Craton: Evidence from petrology and geochemistry of peridotite xenoliths. *Lithos* **101**, 435-452.

Taylor B. and Hayes D. E. (1983) Origin and history of the South China Sea basin. In: Dennis E, Hayes D E, eds. The Tectonic and Geologic Evolution of South Eastern Asian seas and islands. *AGU Geophys Monogr*, 23–56.

Trail D., Watson E. B. and Tailby N. D. (2012) Ce and Eu anomalies in zircon as proxies for the oxidation state of magmas. *Geochim. Cosmochim. Acta* **97**, 70-87.

Tu K., Flower M. F., Carlson R. W., Zhang M. and Xie G. (1991) Sr, Nd, and Pb isotopic compositions of Hainan basalts (south China): implications for a subcontinental lithosphere Dupal source. *Geology* **19**, 567-569.

Tu K., Flower M. F., Carlson R. W., Xie G., Chen C. and Zhang M. (1992) Magmatism in the South China Basin. *Chem. Geol.* **97**(1), 47-63.

Vervoort J. D., Patchett P. J., Blichert-Toft J. and Albarède F. (1999) Relationships between Lu–Hf and Sm–Nd isotopic systems in the global sedimentary system. *Earth Planet. Sci. Lett.* **168**, 79-99.

Vroon P., Bergen M. V., White W. and Varekamp J. (1993) Sr-Nd-Pb isotope systematics of the Banda Arc, Indonesia: Combined subduction and assimilation of continental material. *J.Geophys. Res.* **98**, 22349-22366.

Wang X., Li Z., Li X., Li J., Liu Y., Long W., Zhou J. and Wang F. (2011) Temperature, pressure, and composition of the mantle source region of Late Cenozoic basalts in Hainan Island, SE Asia: a consequence of a young thermal mantle plume close to subduction zones? *J. Petrol.* **53**, 177-233.

Wang X., Li Z., Li X., Li J., Xu. Y. and Li X. (2013) Identification of an ancient mantle reservoir and young recycled materials in the source region of a young mantle plume: Implications for potential linkages between plume and plate tectonics. *Earth Planet. Sci. Lett.* **377**, 248–259.

Weaver B. L. (1991) The origin of ocean island basalt end-member compositions: trace element and isotopic constraints. *Earth Planet. Sci. Lett.* **104**, 381-397.

Willbold M. and Stracke A. (2006) Trace element composition of mantle end-members: Implications for recycling of oceanic and upper and lower continental crust. *Geochem. Geophys. Geosyst*. **7**.

Wittig N., Pearson D. G., Downes H. and Baker J. A. (2009) The U, Th and Pb elemental and isotope compositions of mantle clinopyroxenes and their grain boundary contamination derived from leaching and digestion experiments. *Geochim. Cosmochim. Acta* **73**, 469-488.

Wittig N., Pearson D. G., Duggen S., Baker J. A. and Hoernle K. (2010) Tracing the metasomatic and magmatic evolution of continental mantle roots with Sr, Nd, Hf and and Pb isotopes: A case study of Middle Atlas (Morocco) peridotite xenoliths. *Geochim. Cosmochim. Acta* **74**, 1417-1435.

Wood D. A. (1979) A variably veined suboceanic upper mantle—Genetic significance for mid-ocean ridge basalts from geochemical evidence. *Geology* **7**, 499-503.

Woodhead J. D. and Fraser D. G. (1985) Pb, Sr and 10Be isotopic studies of volcanic rocks from the Northern Mariana Islands. Implications for magma genesis and crustal recycling in the Western Pacific. *Geochim. Cosmochim. Acta* **49**, 1925-1930.

672 Workman R. K., Hart S. R., Jackson M., Regelous M., Farley K. A., Blusztajn J., Kurz
673 M. and Staudigel H. (2004) Recycled metasomatized lithosphere as the origin of
674 the Enriched Mantle II (EM2) end-member: Evidence from the Samoan Volcanic
675 Chain. *Geochem. Geophys. Geosyst*. **5**.
676 Wyllie P. J. (1970) Ultramafic rocks and upper mantle, *Mineral. Soc. Am. Spec. Pap.*
677 **3**, 3-32.
678 Xu X., O'Reilly S. Y., Griffin W. and Zhou X. (2003) Enrichment of upper mantle
679 peridotite: petrological, trace element and isotopic evidence in xenoliths from SE
680 China. *Chem. Geol.* **198**, 163-188.
681 Xu Y., Sun M., Yan W., Liu Y., Huang X. and Chen X. (2002) Xenolith evidence for
682 polybaric melting and stratification of the upper mantle beneath South China. *J.*
683 *Asian Earth Sci.* **20**, 937-954.
684 Yaxley G. M. and Sobolev A. V. (2007) High-pressure partial melting of gabbro and
685 its role in the Hawaiian magma source. *Contrib. Mineral. Petrol.* **154**, 371-383.
686 Yan P., Deng H., Liu H., Zhang Z. and Jiang Y. (2006) The temporal and spatial
687 distribution of volcanism in the South China Sea region. *J. Asian Earth Sci.* **27**(5),
688 647-659.
689 Yan Q. and Shi X. (2007) Hainan mantle plume and the formation and evolution of the
690 South China Sea. *Geological Journal of China Universities* **13**, 311-322.
691 Yan Q., Shi X., Wang K., Bu W. and Xiao L. (2008) Major element, trace element, and
692 Sr, Nd and Pb isotope studies of Cenozoic basalts from the South China Sea.
693 *Science in China Series D: Earth Sciences* **51**, 550-566.

694 Yan Q., Castillo P., Shi X., Wang L., Liao L. and Ren J. (2015) Geochemistry and
695 petrogenesis of volcanic rocks from Daimao Seamount (South China Sea) and their
696 tectonic implications. *Lithos* **218**, 117-126.
697 Yang Y., Zhang H., Chu Z., Xie L. and Wu F. (2010) Combined chemical separation
698 of Lu, Hf, Rb, Sr, Sm and Nd from a single rock digest and precise and accurate
699 isotope determinations of Lu–Hf, Rb–Sr and Sm–Nd isotope systems using Multi-
700 Collector ICP-MS and TIMS. *Int. J. Mass Spectrom.* **290**, 120-126.
701 Yu J., O'Reilly S. Y., Zhang M., Griffin W. and Xu X. (2006) Roles of melting and
702 metasomatism in the formation of the lithospheric mantle beneath the Leizhou
703 Peninsula, South China. *J. Petrol.* **47**, 355-383.
704 Zanetti A., Vannucci R., Bottazzi P., Oberti R. and Ottolini L. (1996) Infiltration
705 metasomatism at Lherz as monitored by systematic ion-microprobe investigations
706 close to a hornblendite vein. *Chem. Geol.* **134**(1), 113-133.
707 Zeng G., Chen L.-H., Hu S.-L., Xu X.-S., and Yang L.-F. (2013) Genesis of Cenozoic
708 low-Ca alkaline basalts in the Nanjing basaltic field, eastern China: The case for
709 mantle xenolith-magma interaction: *Geochem. Geophys. Geosyst*. **14**, 1660-1677.
710 Zhang M., Tu K., Xie G., and Flower M. F. (1996) Subduction-modified subcontinental
711 mantle in South China: Trace element and isotope evidence in basalts from Hainan
712 Island. *Chinese Journal of Geochemistry* **15**(1), 1-19.
713 Zhao D. (2004) Global tomographic images of mantle plumes and subducting slabs:
714 insight into deep Earth dynamics. *Phys. Earth Planet In.* **146**, 3-34.
715 Zheng J., Griffin W. L., O'Reilly S. Y., Yang J., Li T., Zhang M., Zhang R. Y. and Liou

J. G. (2006) Mineral chemistry of peridotites from Paleozoic, Mesozoic and Cenozoic lithosphere: constraints on mantle evolution beneath eastern China. *J. Petrol.* **47**, 2233-2256.

Zindler A. and Hart S. (1986) Chemical geodynamics. *Annual review of earth and planetary sciences* **14**, 493-571.

Zhou X. M. and Li W. X. (2000) Origin of Late Mesozoic igneous rocks of southeastern China: implications for lithosphere subduction and underplating of mafic magma. *Tectonophysics* **326**, 269–287.

Zou H., Zindler A., Xu X. and Qi Q. (2000) Major, trace element, and Nd, Sr and Pb isotope studies of Cenozoic basalts in SE China: mantle sources, regional variations, and tectonic significance. *Chem. Geol.* **171**, 33-47.

Zou H. and Fan Q. (2010) U–Th isotopes in Hainan basalts: Implications for sub-asthenospheric origin of EM2 mantle endmember and the dynamics of melting beneath Hainan Island. *Lithos* **116**(1), 145-152.

Figure captions

Fig. 1. (a) Distribution of the Cenozoic intraplate volcanism in Southeast Asia (after Wang et al. (2011)). (b) Distribution of the Cenozoic intraplate volcanism in the Leizhou Peninsula and Hainan Island and sampling locations of the late Cenozoic volcanic rocks in the Leizhou Peninsula.

Fig. 2. (a) Layered structures of the volcanic lavas in the Leizhou Peninsula. (b) Porous and ropy structures at the surface of lava layers. (c-d) Photomicrographs showing

intergranular textures, with phenocrysts and microlites of olivine, clinopyroxene and magnetite aggregated between euhedral plagioclase laths.

Fig. 3. TAS diagram (a) and selected $Mg^{\#}$ variation diagrams (b-h). These volcanic rocks have experienced varying extent of fractional crystallization with the liquidus minerals dominated by olivine and clinopyroxene. The volcanic rocks from Huoju are more evolved with higher SiO_2 and lower $Mg^{\#}$ than those from Jiujiang and Tianyang. For comparison, the compiled major element compositions and Cr and Ni contents of Cenozoic basaltic rocks from the Hainan Island are also plotted (Tu et al., 1991; Flower et al., 1992; Zou and Fan, 2010; Ho et al., 2000; Wang et al., 2011).

Fig. 4. (a) Chondrite-normalized REE patterns of the volcanic rocks from the Leizhou Peninsula. (b) Primitive mantle-normalized multiple incompatible element abundances of these rocks. For comparison, average compositions of present-day OIB (Sun and McDonough, 1989) and upper continental crust (UCC) (Rudnick and Gao, 2003) are plotted. The sample ZC11-02 with negative Ce anomaly also has negative Zr and Hf anomalies as the result of excess zircon crystallization.

Fig. 5. Distinct $[Nb/Th]_N$ and $[Ta/U]_N$ (a) (primitive mantle normalized Nb/Th and Ta/U ratios to show the Nb and Ta anomalies) and Sr/Sr^* and Eu/Eu^* (b) ($Sr/Sr^*= 2*Sr_{PM}/[Pr_{PM} + Nd_{PM}]$ and $Eu/Eu^*= 2*Eu_{PM}/[Sm_{PM} + Gd_{PM}]$ to show the Sr and Eu anomalies) between the samples from Huoju and Jiujiang and Tianyang. For comparison, the compositions of Cenozoic basalts from the Hainan Island (Tu et al., 1991; Flower et al., 1992; Zou and Fan, 2010; Ho et al., 2000; Wang et al., 2011) and the average compositions of present-day OIB, both normal (N-type) and enriched (E-

type) MORB (Sun and McDonough, 1989) and UCC (Rudnick and Gao, 2003) are also plotted.

Fig. 6. Sr-Nd-Pb-Hf isotope co-variations of the volcanic rocks from the Leizhou Peninsula. The terrestrial array in the Nd-Hf isotopic space is from Vervoort et al. (1999). Northern Hemisphere Reference Line (NHRL) is from Hart (1984). The Sr-Nd-Pb isotope compositions of Cenozoic basalts from the Hainan Island (Tu et al., 1991; Flower et al., 1992; Zou and Fan, 2010; Ho et al., 2000; Wang et al., 2011) and the South China Sea Basin (SCSB; Tu et al., 1992; Yan et al., 2008, 2015), the Pb isotope compositions of the Central Indian Ridge (CIR) MORB (Mahoney et al., 1989) and average Java trench sediment that is largely mature continent derived (Plank and Langmuir, 1998) are also plotted for comparison.

Fig. 7. Modelling of crustal contamination in the SiO_2 vs. $^{87}Sr/^{86}Sr$ diagram. The sample from Jiujiang with lowest SiO_2 (47.78 wt. %) was assumed as the basaltic melt unaffected by crustal contaminations. UCC material with 66.6 wt.% SiO_2, 327 ppm Sr (Rudnick and Gao, 2003) and $^{87}Sr/^{86}Sr$ value of 0.7173 (Plank and Langmuir, 1998) is modelled to mix with the basaltic melt by variable extents. The modelling results show that the volcanic rocks in the Leizhou Peninsula are apparently off the mixing trend. To generate the Huoju samples with 54.87-61.21 wt.% SiO_2, as high as ~38-70% UCC materials are needed to assimilate with the basaltic melt, which would generate melts with high $^{87}Sr/^{86}Sr$ values of ~0.7071-0.7116, much higher than the $^{87}Sr/^{86}Sr$ values (0.703882-0.704888) of the Huoju samples.

Fig. 8. In contrast with the positive correlation between Sr/Sr^* and SiO_2 and negative

correlations between Sr/Sr^* and $[La/Sm]_N$, Nb/U and Zr/Hf in the Cenozoic volcanic rocks in the Hainan Island, the samples from the Leizhou Peninsula have negative correlation of Sr/Sr^* with SiO_2, and positive correlations of Sr/Sr^* with $[La/Sm]_N$, Nb/U and Zr/Hf. Hence, the positive Sr anomalies in the volcanic rocks from the Leizhou Peninsula cannot be explained by the involvement of the recycled oceanic crust materials in the mantle source region. The positive Sr anomalies ($Sr/Sr^* > 1$) of the volcanic rocks from the Leizhou peninsula are consistent with the incompatible element enrichment in the mantle source (See text for details).

Fig. 9. Distinct Pb/Ce and Sr/Sr^* trends between Jiujiang/Tianyang and Huoju rock suites. For comparison, the compositions of Cenozoic basalts from the Hainan Island are also plotted (Tu et al., 1991; Flower et al., 1992; Zou and Fan, 2010; Ho et al., 2000; Wang et al., 2011). The Jiujiang and Tianyang samples show low Pb/Ce but high Sr/Sr^*, which is similar to the amphiboles in the mantle xenoliths (Yu et al., 2006) and is consistent with a low-F melt mantle metasomatism. The Huoju samples and rocks from the Hainan Island show high Pb/Ce and relative low Sr/Sr^*, which is similar to the clinopyroxenes in the mantle xenoliths (Yu et al., 2006) and indicates a mantle metasomatism by recycled UCC materials.

Fig. 10. Correlations of Sr-Nd-Pb-Hf isotope ratios with their respective parent/daughter ratios ($^{87}Rb/^{86}Sr$, $^{147}Sm/^{144}Nd$, $^{238}U/^{204}Pb$ and $^{176}Lu/^{177}Hf$). The positive correlation between Rb/Sr and $^{87}Sr/^{86}Sr$ gives a pseudochron age of 1298 Ma. This age has no geological significance, but is best explained by melting-induced mixing with the pseudochron slope controlled by the compositions of the two endmembers, i.e., a low-F melt metasomatized asthenospheric mantle material with high Sr content, low

Rb/Sr and depleted Sr isotope composition and a recycled UCC material with high Rb/Sr and enriched Sr isotope composition. The samples from Jiujiang and Tianyang with low $^{147}Sm/^{144}Nd$ and $^{176}Lu/^{177}Hf$ and high $^{238}U/^{206}Pb$ have high $^{143}Nd/^{144}Nd$ and $^{176}Hf/^{177}Hf$ and low $^{206}Pb/^{204}Pb$, which is consistent with the characteristics of a recent (or "current") low-F melt metasomatism without enough time for isotope intergrowth. Sample ZC11-02 show the same characteristics with other Jiujiang/Tianyang samples except for its low Zr-Hf-Ce due to excess zircon fractionation (see Fig. 4).

Fig. 11. Trace element modelling of the multiple metasomatic events in the mantle source region of the volcanic rocks in the Leizhou Peninsula. Sr-Nd-Pb-Hf isotopes are not used in these modellings because the recent metasomatic low-F melts should have indistinguishable depleted Sr-Nd-Pb-Hf isotopes with the depleted MORB mantle (DMM). The average La/Yb, Lu/Hf, Ta/U and Nb/Th ratios of the recycled upper continental crust (UCC) materials are calculated using recommended UCC compositions from Rudnick and Gao (2003). The average values of the above element ratios of DMM are calculated using recommended DMM compositions from Salters and Stracke (2004). The low-F melt component is assumed to be represented by an incompatible elements most enriched sample from Jiujiang and Tianyang (JJ11-01). The modelling results show that ~6%-10% recycled UCC materials were mixed with the DMM in the first place. Such recycled UCC material modified mantle was then further metasomatized by the low-F melt by variable extents to generate the ultimate mantle source of the volcanic rocks in the Leizhou Peninsula.

Fig. 12. (a) The paleo-Pacific plate subducted along the present Southeast China coastline in the Mesozoic until exotic terranes (represented by the basement of

continental shelf of East and South China Seas) jammed the trench and ceased the subduction activity at ~ 100 Ma (Niu et al., 2015). UCC material subducted as terrestrial sediment can melt and metasomatize the overlying asthenosphere in the mantle wedge (Johnson and Plank, 2000). (b) After subduction cessation, the Leizhou Peninsula was in an intraplate environment. The asthenospheric mantle beneath Leizhou Peninsula experienced a low-F melt metasomatism. Such low-F melt enriched in incompatible elements and volatiles tended to rise (green arrows) due to buoyancy to metasomatize the overlying asthenospheric mantle that had been pre-modified by a recycling UCC material. The low-F melt can also metasomatize the overlying lithospheric mantle by crystallizing hydrous minerals (e.g. amphibole) and forming garnet pyroxenite, hornblende-pyroxenite and hornblendite veins in the lithospheric mantle (Niu et al., 2002, 2012; Niu and O'Hara, 2003; Niu, 2005). Decompressional melting (red arrows) of such a multiply metasomatized asthenospheric mantle formed the late Cenozoic volcanisms we studied.

Fig. 1

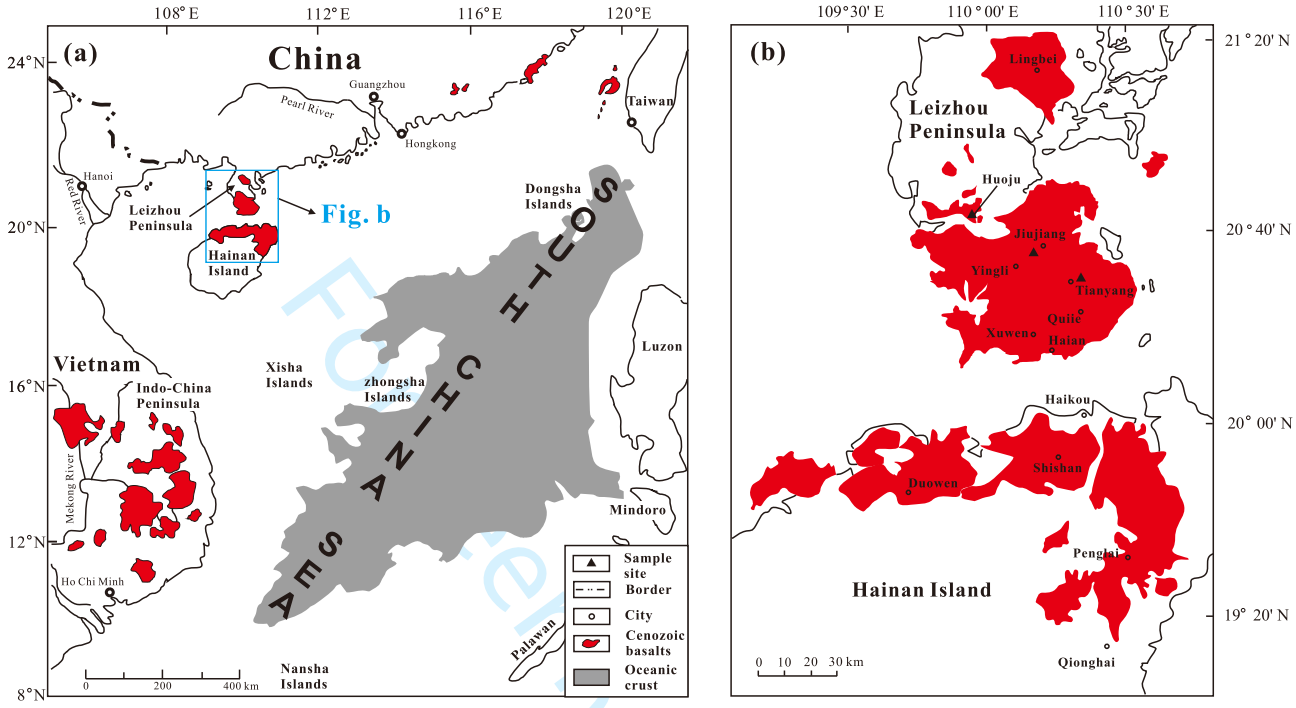

Fig. 2

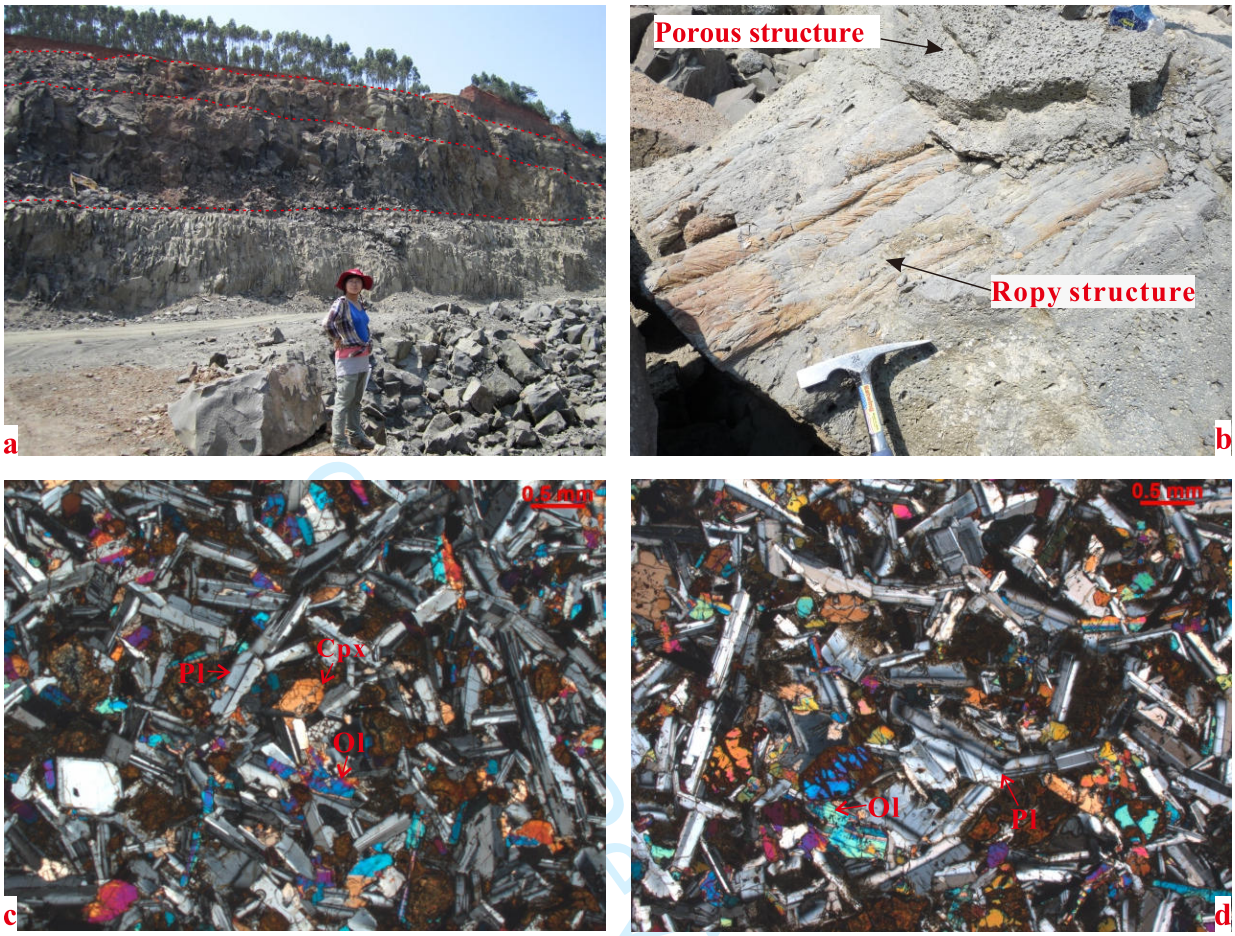

Fig. 3

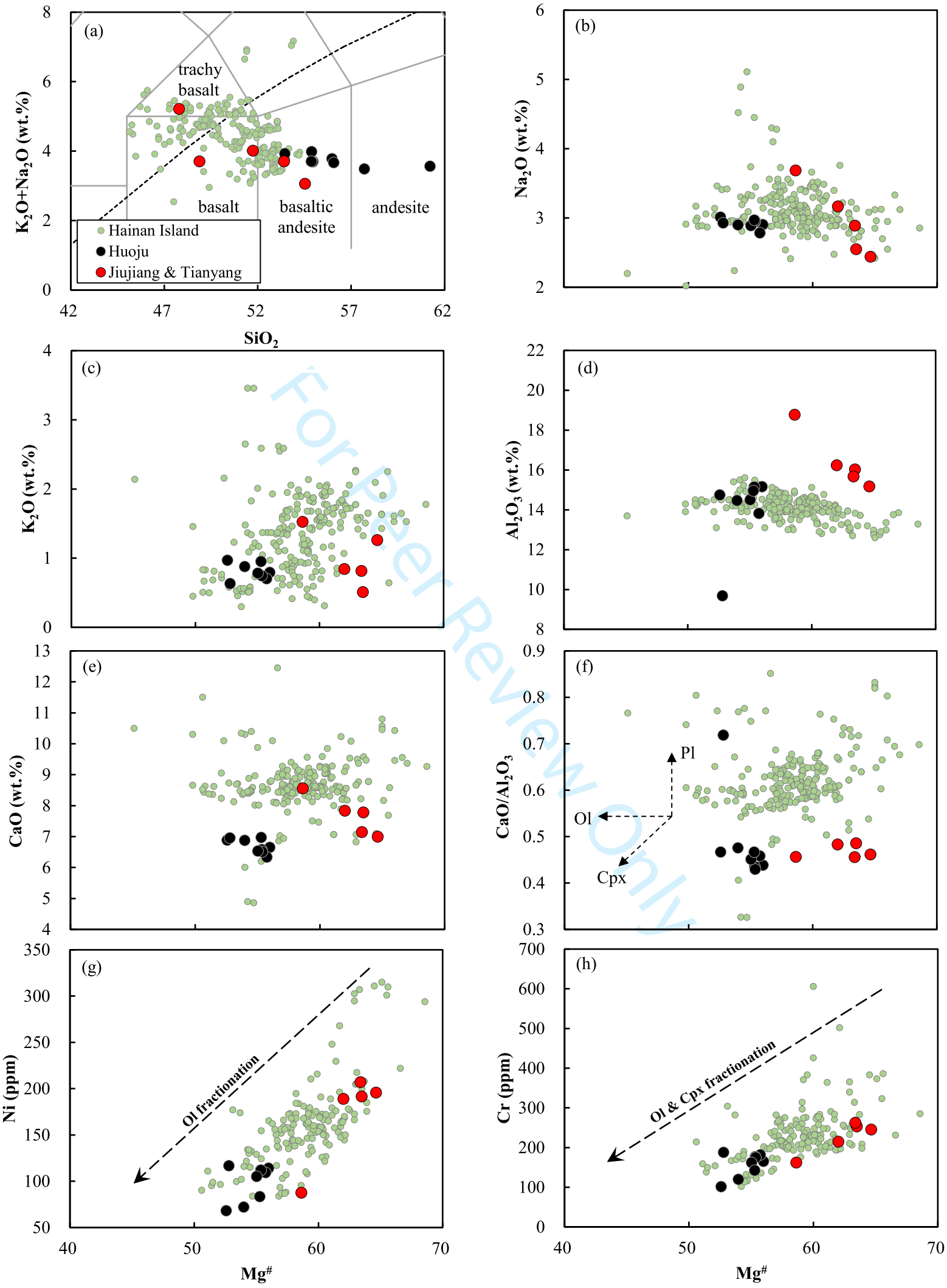

Fig. 4

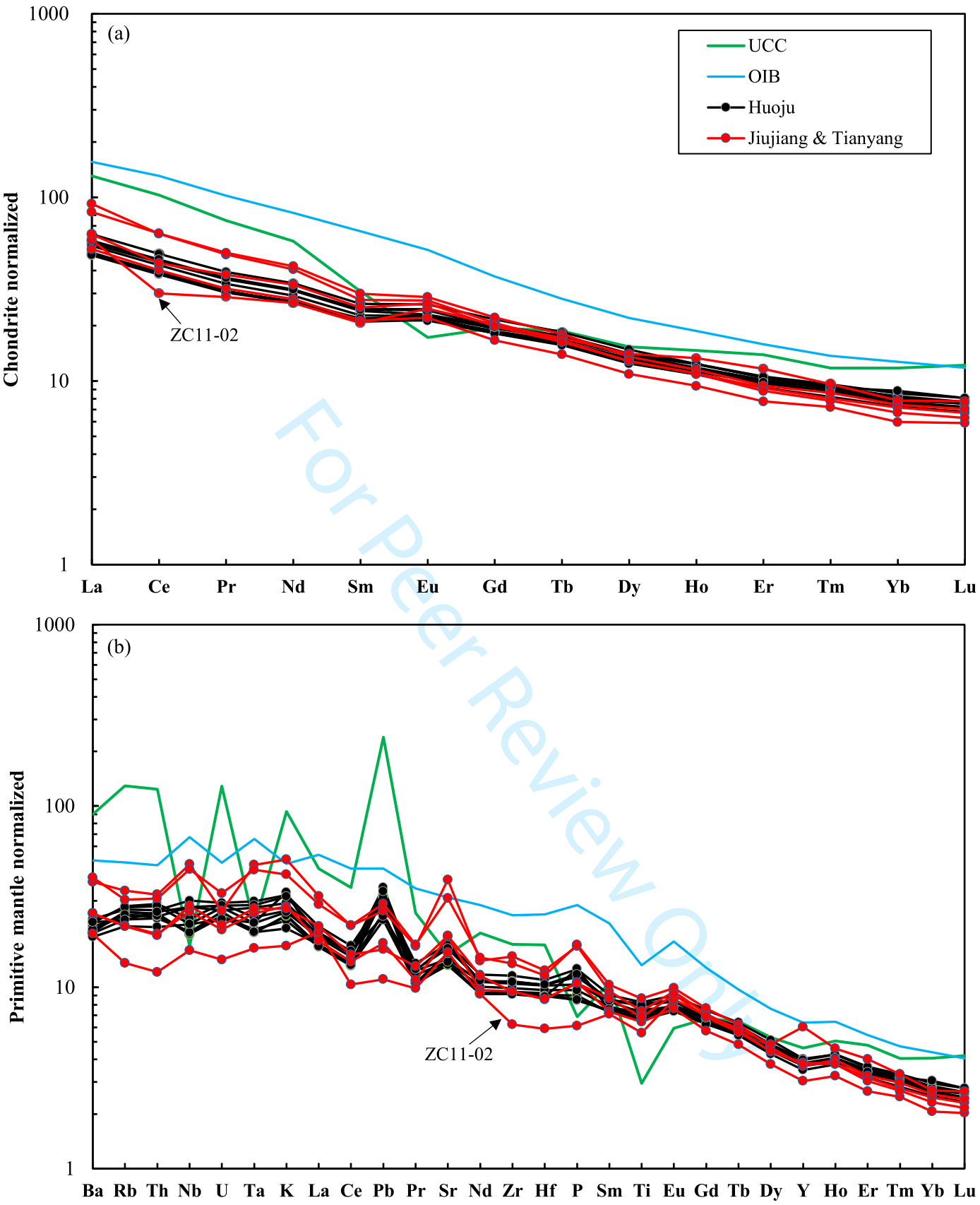

Fig. 5

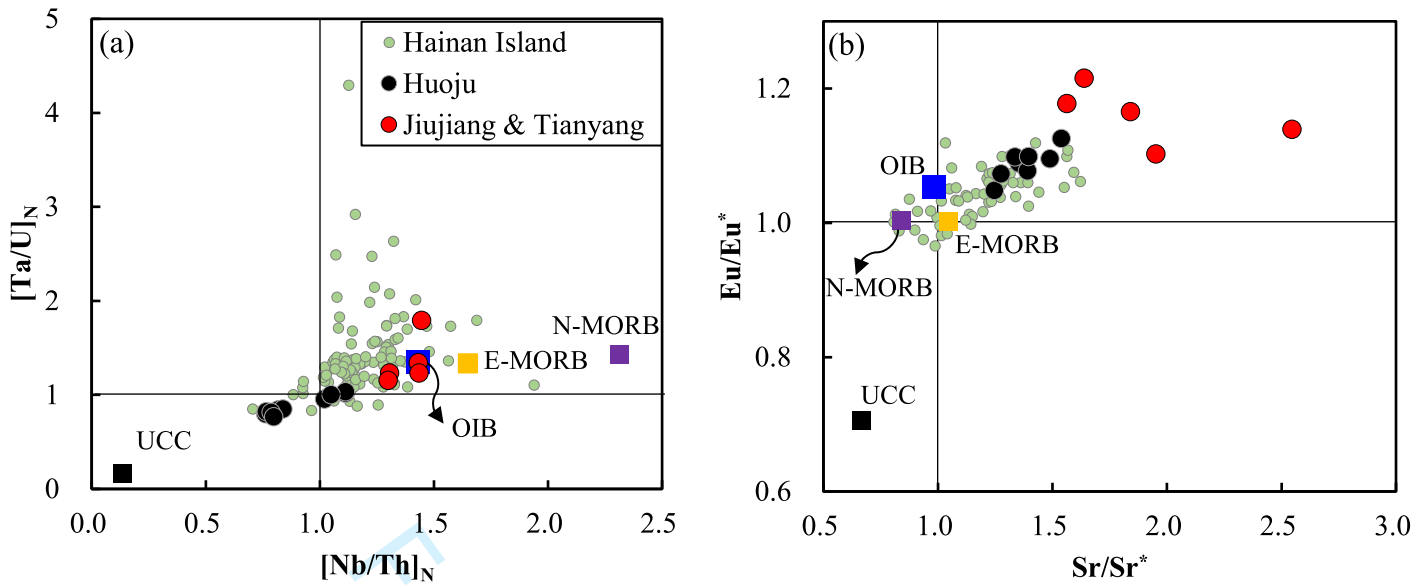

Fig. 6

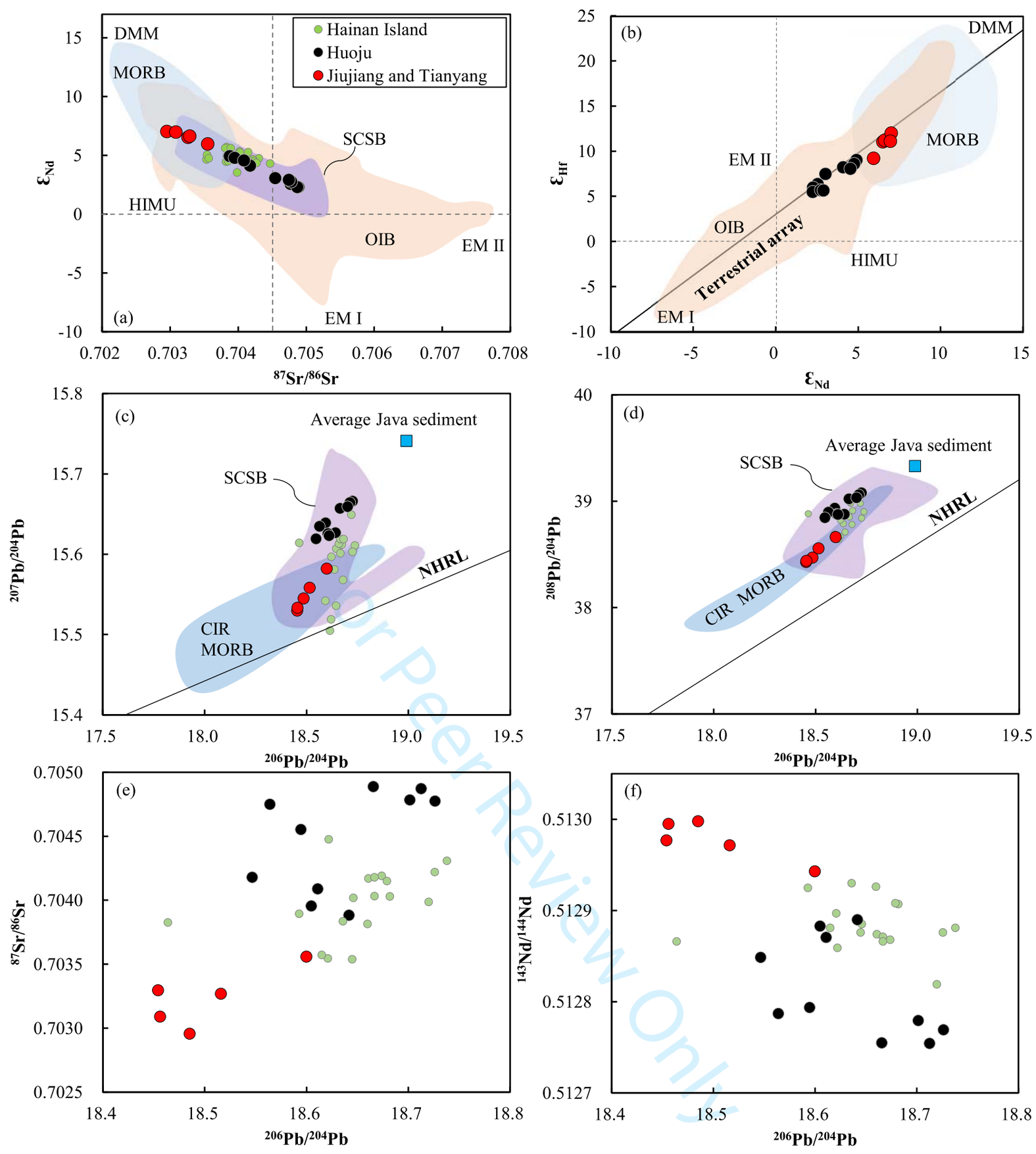

Fig. 7

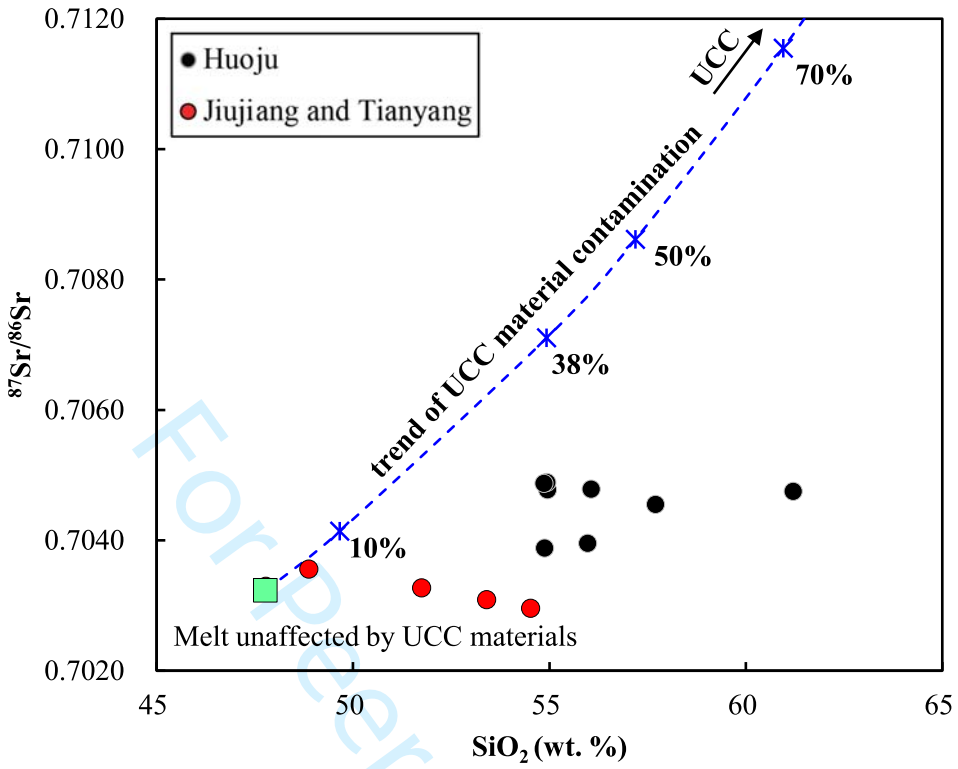

Fig. 8

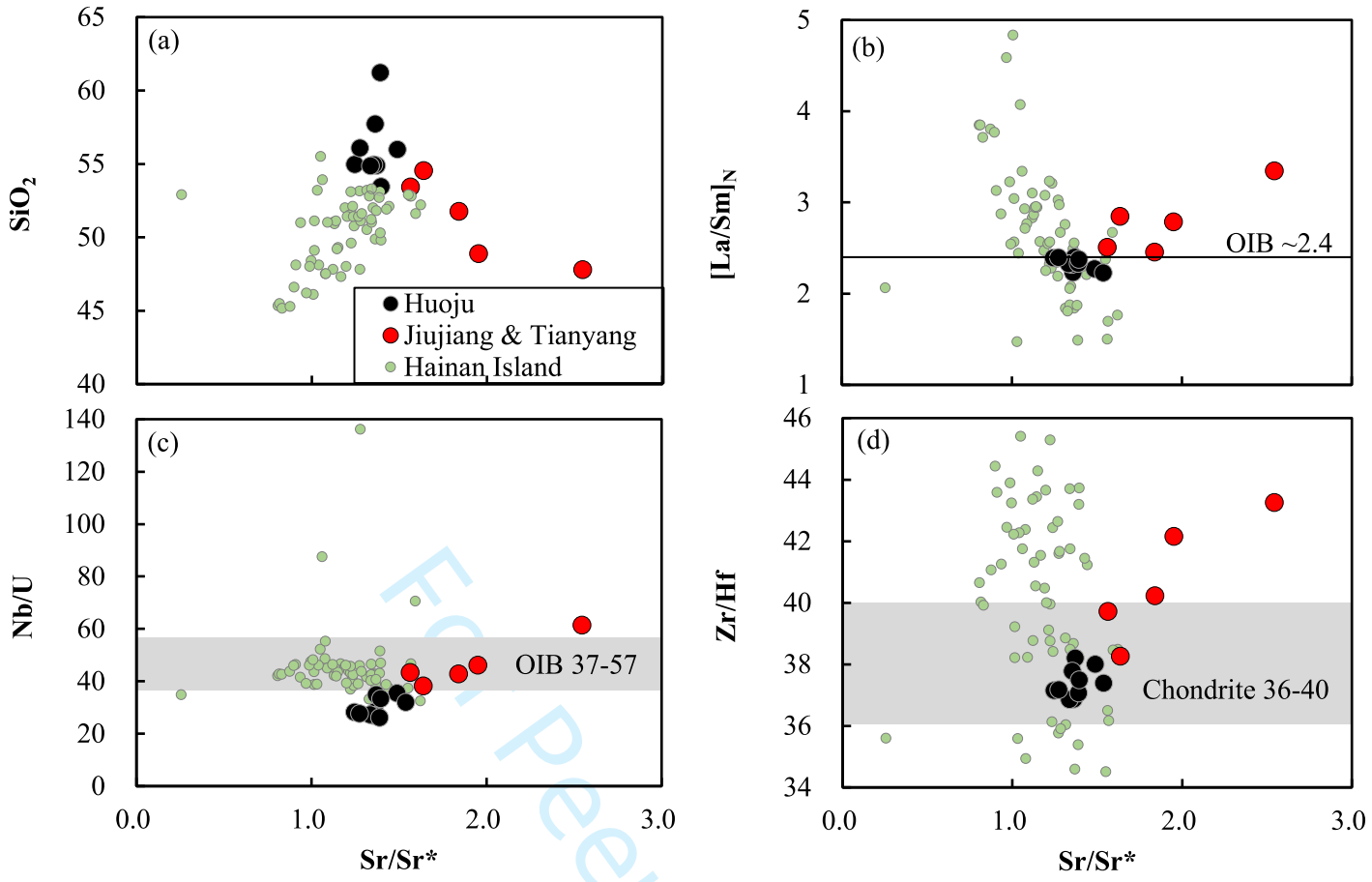

Fig. 9

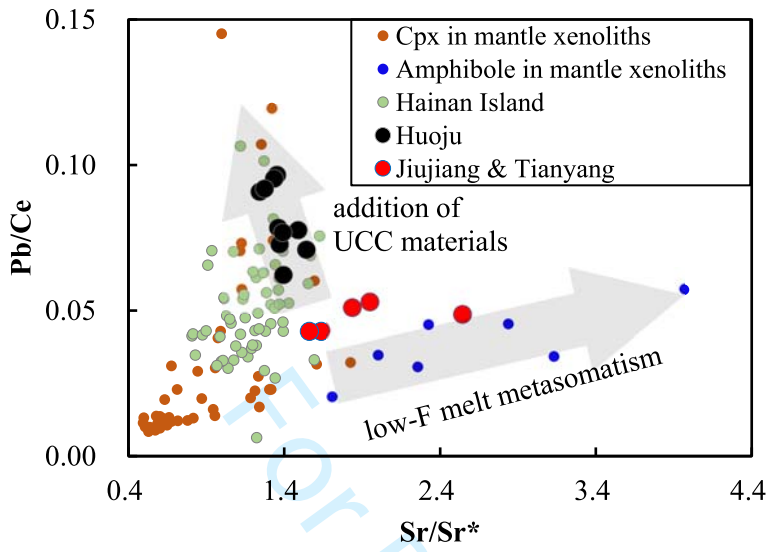

Fig. 10

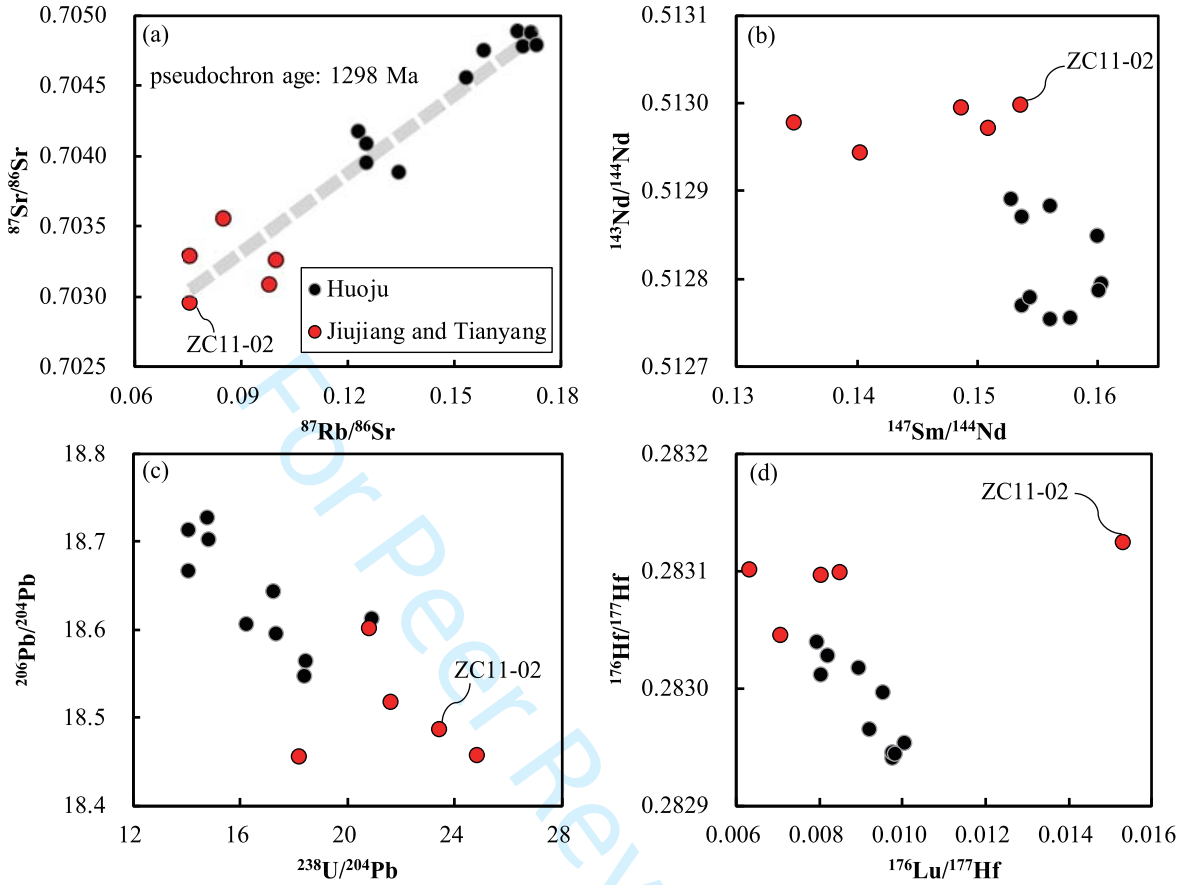

Fig. 11

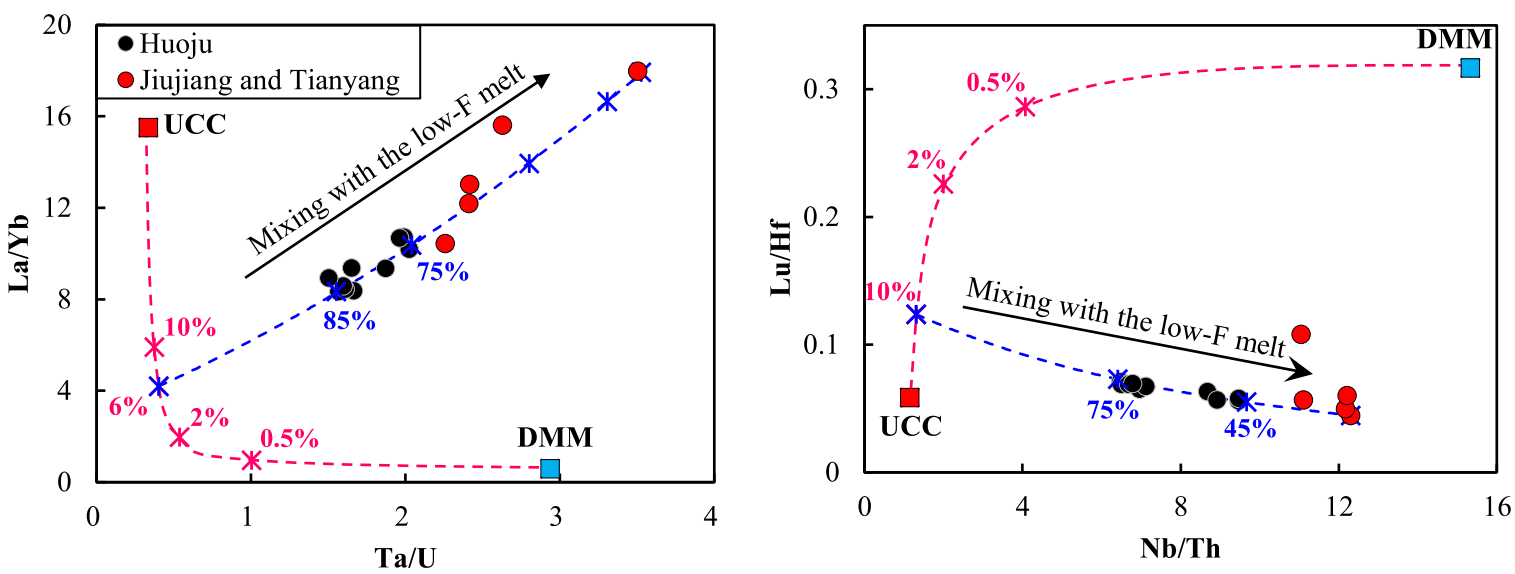

Fig. 12

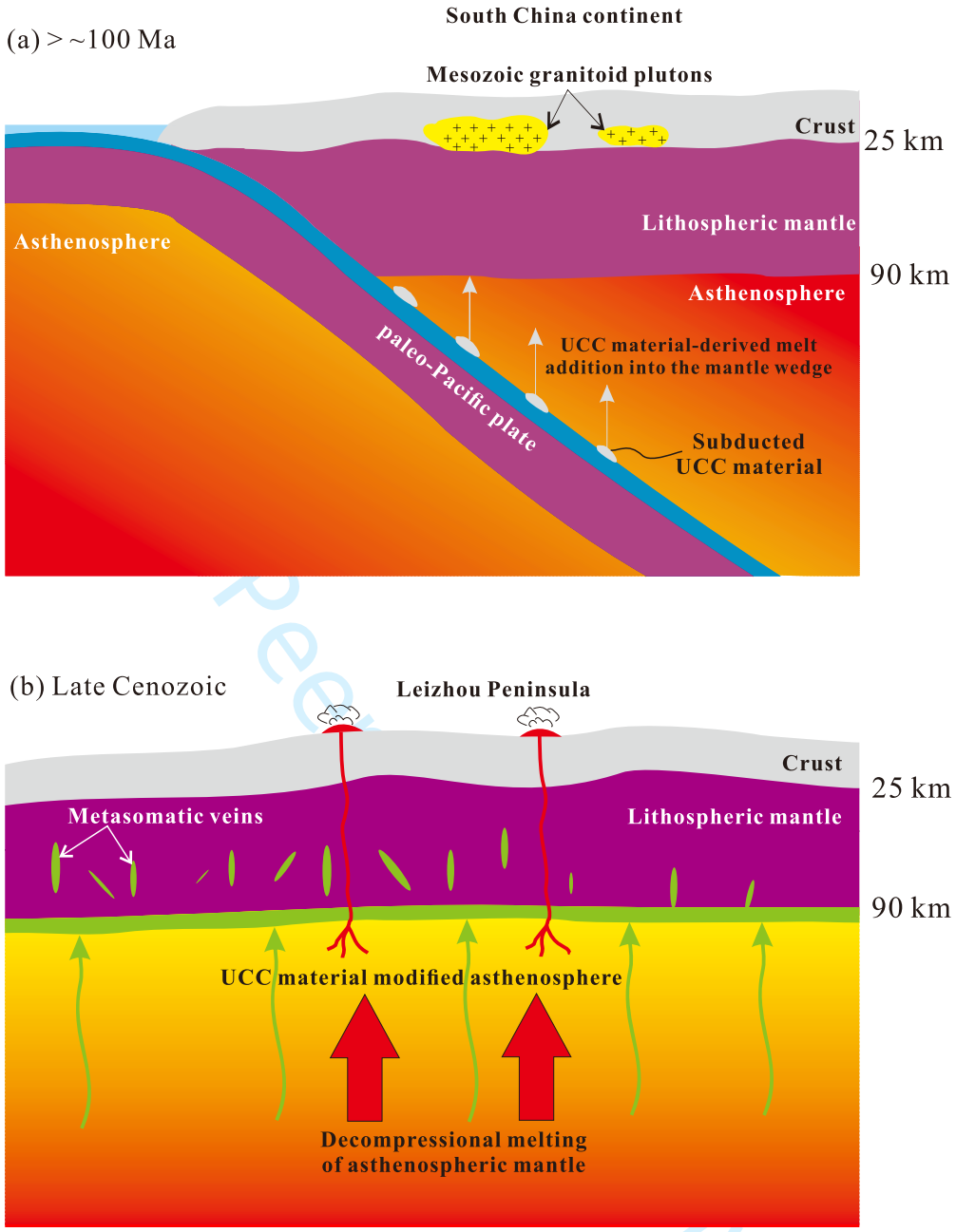
South China continent
(a) > ~100 Ma
Mesozoic granitoid plutons
Crust
25 km
Lithospheric mantle
Asthenosphere
90 km
Asthenosphere
UCC material-derived melt
addition into the mantle wedge
paleo-Pacific plate
Subducted
UCC material
(b) Late Cenozoic
Leizhou Peninsula
Crust
25 km
Metasomatic veins
Lithospheric mantle
90 km
UCC material modified asthenosphere
Decompressional melting
of asthenospheric mantle

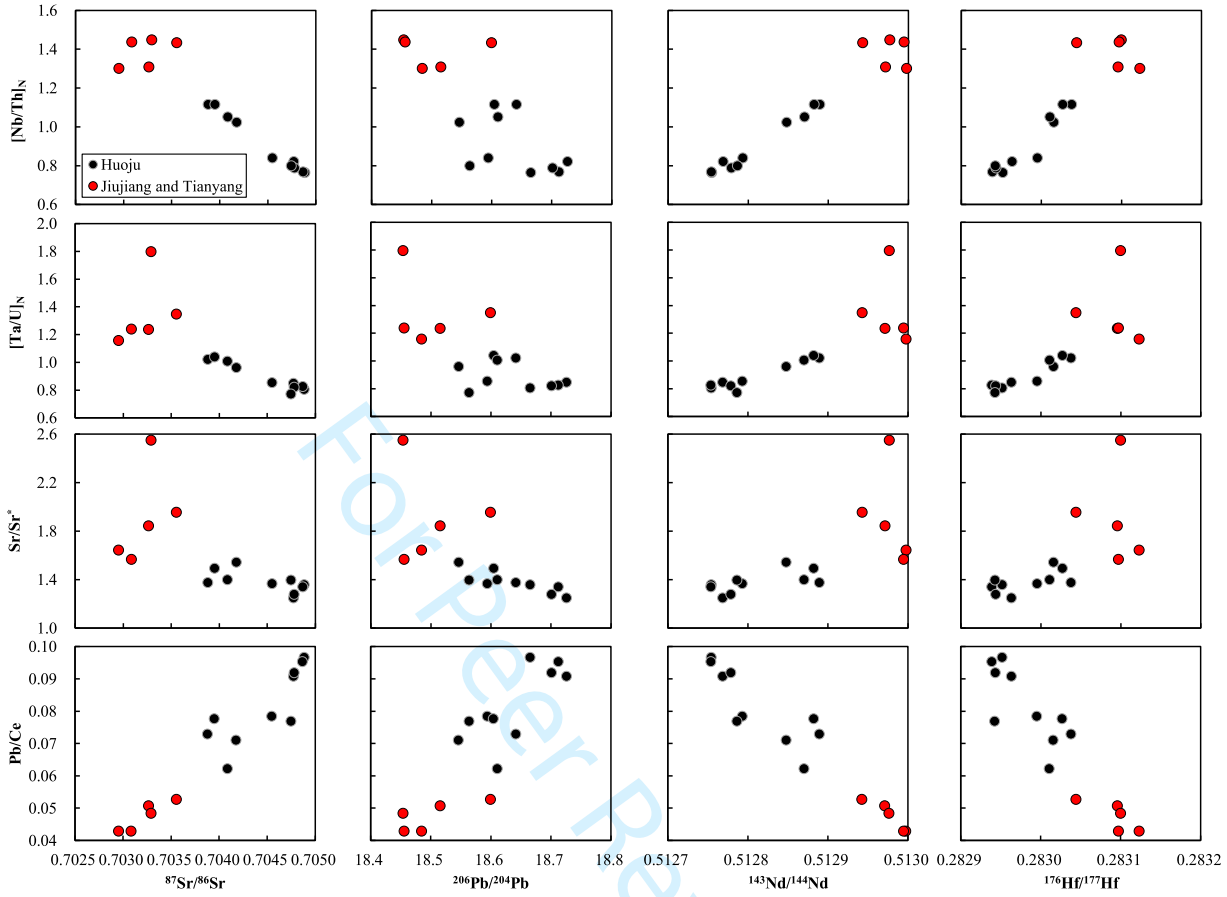

Supplementary Figure 1 Significant correlations of Sr-Nd-Pb-Hf isotope ratios with $[Nb/Th]_N$, $[Ta/U]_N$, Sr/Sr* and Pb/Ce ratios, suggesting that the isotopically enriched component has low $[Nb/Th]_N$, $[Ta/U]_N$ and Sr/Sr* and high Pb/Ce, which is consistent with the contribution of recycled UCC materials in the mantle source regions.

Supplementary Table 1 Major and trace element compositions of the analyzed USGS standard AGV-2 and the volcanic rocks from Leizhou Peninsula

		Huoju										*Jiujiang & Tianyang*				
Sample	AGV-2	HJ11-01	HJ11-03	HJ11-06	HJ11-07	HJ11-09	HJ11-11	HJ11-12	HJ11-13	HJ11-14	HJ11-15	JJ11-01	TY11-01	ZC11-01	ZC11-02	ZC11-03
Lat.		20.77	20.77	20.77	20.77	20.77	20.77	20.77	20.77	20.77	20.77	20.59	20.52	20.52	20.52	20.52
Long.		109.95	109.95	109.95	109.95	109.95	109.95	109.95	109.95	109.95	109.95	110.17	110.31	110.31	110.31	110.31
ICP-OES analyses (wt.%)																
SiO_2	59.48	54.96	54.88	57.71	54.94	55.98	54.87	56.06	61.21		53.45	47.78	51.75	48.88	54.53	53.41
TiO_2	1.07	1.63	1.86	1.51	1.53	1.76	1.55	1.59	1.53		1.83	1.83	1.54	1.94	1.27	1.52
Al_2O_3	17.31	15.16	14.75	13.82	15.11	14.47	15.15	14.50	9.68		14.95	18.77	16.23	15.17	16.03	15.67
TFe_2O_3	6.72	10.06	10.27	9.88	10.56	9.78	10.52	10.26	10.32		10.44	9.95	10.01	10.71	9.05	9.45
MnO	0.10	0.11	0.10	0.10	0.11	0.10	0.11	0.11	0.11		0.09	0.13	0.11	0.12	0.11	0.10
MgO	1.79	5.81	5.17	5.65	5.94	5.21	5.93	5.70	5.24		5.86	6.41	7.43	8.90	7.15	7.43
CaO	5.08	6.65	6.89	6.34	6.58	6.88	6.51	6.54	6.96		6.98	8.56	7.84	7.00	7.79	7.14
Na_2O	4.20	2.91	3.01	2.78	2.94	2.90	2.96	2.89	2.93		2.97	3.69	3.17	2.44	2.55	2.89
K_2O	2.95	0.80	0.97	0.70	0.75	0.88	0.74	0.78	0.64		0.95	1.53	0.84	1.26	0.51	0.82
P_2O_5	0.51	0.23	0.27	0.18	0.19	0.25	0.20	0.21	0.19		0.26	0.37	0.23	0.37	0.13	0.23
LOI	0.41	1.07	1.18	0.66	0.72	1.15	0.83	0.72	0.53		1.62	0.41	0.27	2.70	0.27	0.75
Total	99.62	99.37	99.37	99.35	99.36	99.36	99.36	99.36	99.34		99.39	99.43	99.41	99.49	99.38	99.41
$Mg^{\#}$	37.18	55.98	52.58	55.74	55.33	53.98	55.37	55.02	52.79		55.29	58.63	62.01	64.65	63.49	63.38
ICP-MS analyses (ppm)																
Sc	12.4	17.5	17.5	18.1	18	17.8	18	17.8	17.6	18.2	17.4	18.2	17.8	18.8	17.7	17.9
V	115	128	144	132	129	144	128	130	124	141	139	154	129	154	125	135
Cr	15	165	102	182	177	120	175	162	188	175	143	162	215	246	253	262
Mn	726	1018	952	971	1001	979	999	989	1038	945	826	1070	973	1158	1050	914
Co	14.3	39.1	36.7	39.3	39.3	36.5	38.5	38.2	39	39.3	38	37.4	42.4	47.7	48.2	42.3
Ni	17	114	68	109	112	72	112	105	117	98	83	87	189	196	192	207
Cu	45	44	34	42	41	33	41	43	41	34	36	52	72	52	54	53
Zn	87	112	107	106	107	105	108	108	103	103	102	87	90	99	82	90
Ga	18.7	19	19.3	18.7	18.7	18.9	18.4	18.3	18.4	18.2	18.5	19.5	17.5	17.9	16.3	17.5
Rb	62.0	17.7	17	15	16.5	15.8	16.6	17.5	15.9	13.8	15	21.6	13.9	19.3	8.6	13.8
Sr	639	303	365	283	284	363	279	292	290	324	345	827	400	653	329	406
Y	17.8	18.1	18.3	17.2	17.3	17.3	17.1	18.1	16.8	15.9	16.9	17.5	13.8	16.7	28	17.2
Zr	220	117	130	106	104	121	103	111	103	102	120	166	106	151	70	106
Nb	13.2	17	21	14.5	14	19.7	14	15.9	14.3	15.9	19.7	34	18.6	32	11.4	20
Cs	1.125	0.3	0.22	0.172	0.23	0.24	0.25	0.24	0.21	0.147	0.144	0.134	0.21	0.13	0.157	0.147
Ba	1100	158	166	138	143	150	141	160	145	132	160	266	178	282	138	179
La	36.4	13.6	14.9	11.5	11.7	13.3	11.6	12.9	11.8	11.5	13.8	21.9	12.4	19.7	13.9	14.9
Ce	66.0	27.8	30.1	23.3	23.7	27.2	23.6	26.2	23.9	23.5	28.1	38.8	24.6	39	18.4	26.9
Pr	7.64	3.4	3.73	2.88	2.93	3.41	2.92	3.22	2.94	2.92	3.46	4.64	3.02	4.74	2.72	3.6
Nd	28.6	14.5	15.9	12.5	12.5	14.6	12.5	13.6	12.4	12.7	14.7	18.9	13.1	19.7	12.4	15.6
Sm	5.11	3.69	4.02	3.32	3.26	3.78	3.22	3.48	3.29	3.35	3.75	4.23	3.26	4.58	3.16	3.85
Eu	1.46	1.33	1.51	1.27	1.25	1.42	1.25	1.31	1.24	1.31	1.4	1.59	1.28	1.66	1.44	1.53
Gd	4.35	4.08	4.45	3.84	3.78	4.16	3.74	3.97	3.74	3.73	4.04	4.25	3.42	4.56	4.16	4.08
Tb	0.606	0.662	0.690	0.616	0.6	0.647	0.608	0.636	0.593	0.586	0.637	0.623	0.522	0.674	0.6	0.609
Dy	3.21	3.59	3.77	3.36	3.39	3.51	3.36	3.54	3.29	3.16	3.49	3.25	2.77	3.44	3.57	3.27
Ho	0.632	0.701	0.699	0.666	0.668	0.669	0.659	0.697	0.637	0.615	0.664	0.623	0.532	0.653	0.754	0.618
Er	1.69	1.75	1.73	1.67	1.68	1.63	1.65	1.74	1.60	1.52	1.63	1.51	1.28	1.56	1.93	1.46
Tm	0.251	0.245	0.239	0.231	0.233	0.221	0.234	0.236	0.226	0.209	0.22	0.205	0.184	0.22	0.245	0.199
Yb	1.58	1.46	1.39	1.37	1.4	1.3	1.37	1.50	1.33	1.23	1.29	1.22	1.02	1.26	1.33	1.14
Lu	0.244	0.205	0.19	0.193	0.196	0.184	0.193	0.205	0.192	0.173	0.181	0.17	0.15	0.179	0.197	0.16
Hf	5.14	3.16	3.39	2.86	2.76	3.18	2.8	2.98	2.77	2.74	3.19	3.83	2.64	3.59	1.83	2.67
Ta	0.802	0.999	1.22	0.854	0.819	1.13	0.826	0.924	0.826	0.932	1.16	1.94	1.05	1.82	0.673	1.12
Pb	12.43	2.53	2.19	1.83	2.29	2.11	2.24	2.40	1.84	1.67	1.75	1.88	1.24	2.05	0.79	1.15
Th	5.97	2.45	2.26	2.04	2.17	2.09	2.15	2.38	2.11	1.83	2.21	2.76	1.68	2.62	1.03	1.64
U	1.890	0.605	0.613	0.513	0.523	0.557	0.513	0.579	0.549	0.498	0.593	0.554	0.436	0.692	0.298	0.463

Supplementary Table 2 Sr, Nd, Pb and Hf isotope data of the USGS standards and the volcanic rocks in Leizhou Peninsula

Sample	$^{87}Sr/^{86}Sr$ (± 2σ)	$^{143}Nd/^{144}Nd$ (± 2σ)	εNd	$^{206}Pb/^{204}Pb$	$^{207}Pb/^{204}Pb$	$^{208}Pb/^{204}Pb$	$^{176}Hf/^{177}Hf$ (± 2σ)	εHf
				USGS standards				
AGV-2	0.703980 ± 8	0.512771 ± 8		18.845	15.613	38.527	0.282938 ± 5	
BCR-2	0.705010 ± 7	0.512612 ± 9		18.752	15.622	38.712	0.282840 ± 5	
				Huoju				
HJ11-01	0.704775 ± 8	0.512769 ± 8	2.6	18.727	15.666	39.077	0.282964 ± 9	6.3
HJ11-03	0.703882 ± 14	0.512890 ± 9	4.9	18.642	15.627	38.877	0.283039 ± 8	9.0
HJ11-06	0.704551 ± 8	0.512794 ± 9	3.0	18.595	15.639	38.934	0.282996 ± 8	7.5
HJ11-07	0.704888 ± 7	0.512755 ± 10	2.3	18.666	15.657	39.019	0.282952 ± 6	5.9
HJ11-09	0.703954 ± 8	0.512883 ± 10	4.8	18.605	15.626	38.876	0.283027 ± 6	8.6
HJ11-11	0.704871 ± 8	0.512754 ± 8	2.3	18.713	15.664	39.058	0.282939 ± 5	5.5
HJ11-12	0.704783 ± 7	0.512779 ± 7	2.8	18.702	15.659	39.031	0.282944 ± 6	5.6
HJ11-13	0.704749 ± 9	0.512787 ± 7	2.9	18.564	15.635	38.894	0.282943 ± 7	5.6
HJ11-14	0.704179 ± 6	0.512849 ± 9	4.1	18.547	15.619	38.842	0.283016 ± 5	8.2
HJ11-15	0.704088 ± 8	0.512871 ± 9	4.5	18.611	15.623	38.874	0.283011 ± 6	8.0
				Jiujiang & Tianyang				
TY11-01	0.703267 ± 6	0.512972 ± 7	6.5	18.516	15.558	38.555	0.283096 ± 5	11.0
JJ11-01	0.703295 ± 8	0.512977 ± 9	6.6	18.454	15.530	38.425	0.283100 ± 6	11.1
ZC11-01	0.703557 ± 7	0.512943 ± 8	6.0	18.600	15.582	38.661	0.283045 ± 6	9.2
ZC11-02	0.702955 ± 7	0.512998 ± 11	7.0	18.485	15.545	38.469	0.283124 ± 6	12.0
ZC11-03	0.703088 ± 8	0.512995 ± 8	8.0	18.456	15.533	38.438	0.283098 ± 7	11.1

$\varepsilon Nd = (^{143}Nd/^{144}Nd_{sample}/^{143}Nd/^{144}Nd_{CHUR} - 1) \times 10000$, $^{143}Nd/^{144}Nd_{CHUR} = 0.512638$ (Bouvier et al., 2008).

$\varepsilon Hf = (^{176}Hf/^{177}Hf_{sample}/^{176}Hf^{177}Hf_{CHUR} - 1) \times 10000$, $^{176}Hf^{177}Hf_{CHUR} = 0.282772$ (Blichert-Toft and Albarède, 1997).

Supplementary Table 3 Compiled bulk-rock compositional data for the Cenozoic volcanic rocks in the Hainan Island

Locality	Hainan Island (Tu et al., 1991 & Flower et al., 1992)													
Sample	HN1	HN2	HN3	HN12	HN27	HN64	HN97	HN98	HN99	HN28	HN32	HN33	HN62	HN54
Rock Type	AB	AB	AB	AB	AB	BS	AB	AB	AB	OT	OT	OT	OT	OT
Major elements (wt. %)														
SiO_2	48.20	49.41	48.89	47.01	47.35	45.71	47.32	47.30	47.27	51.53	50.51	49.87	47.88	49.28
TiO_2	2.22	2.39	2.28	2.48	2.61	2.73	2.65	2.81	2.80	2.56	2.63	2.56	2.58	2.31
$A1_2O_3$	13.30	13.19	13.35	14.46	13.74	13.26	12.94	13.89	13.85	14.50	14.37	14.03	13.97	13.91
TFe_2O_3	12.45	12.17	12.50	12.65	12.52	12.56	12.36	12.64	12.70	11.39	11.13	11.28	11.69	11.57
MnO	0.16	0.15	0.17	0.17	0.18	0.17	0.16	0.17	0.17	0.15	0.15	0.15	0.15	0.15
MgO	9.06	9.60	9.19	7.59	9.04	9.06	9.16	8.19	8.06	7.40	6.97	7.55	8.45	7.94
CaO	6.83	7.10	7.07	9.10	10.09	9.53	8.77	7.47	7.51	9.40	9.21	9.18	8.76	8.63
Na_2O	3.07	3.08	3.05	2.41	2.87	3.22	3.23	3.66	3.39	3.41	3.42	3.28	2.79	2.99
K_2O	2.27	2.10	2.25	1.78	1.72	2.06	1.42	1.67	1.82	2.06	2.14	2.06	1.90	1.73
P_2O_5	0.84	0.76	0.83	0.73	0.64	0.72	0.59	0.70	0.68	0.53	0.60	0.54	0.59	0.51
Total	98.41	99.94	99.58	98.38	100.76	99.02	98.62	98.51	98.25	102.93	101.12	100.49	98.76	99.02
Mg#	62.9	64.5	62.9	58.2	62.5	62.4	63.1	59.9	59.4	57.7	59.1	60.6	60.3	61.3
Trace elements (ppm)														
Sc	17.7	18.8	16.8	21.1	23.9	16.8	18.3	16.8	19.4	23.2	21.1	22.0	17.0	14.3
V	133	140	133	186	221	189	185	153	145	196	206	198	184	178
Cr	365	383	340	207	252	257	206	228	230	275	260	273	183	201
Co	53.0	57.6	58.6	55.4	65.5	54.8	57.6	50.6	53.4	56.2	59.0	53.2	48.8	53.6
Ni	303	311	295	195	177	178	218	216	211	121	108	127	158	158
Cu	39.9	41.2	37.5	53.6	60.7	54.6	42.3	47.4	43.2	65.3	66.0	63.7	51.6	50.9
Zn	150	140	145	125	116	123	123	136	124	119	114	111	121	122
Rb	47.9	44.7	42.9	38.8	37.0	40.6	41.4	53.5	62.4	42.9	46.5	45.4	41.1	34.9
Sr	922	685	929	762	685	776	712	832	772	613	617	609	598	533
Y	29.2	26.4	28.1	30.6	29.1	27.9	26.1	27.4	28.6	25.3	27.4	26.5	27.5	25.1
Zr	332	288	309	250	277	249	257	298	288	222	234	225	241	206
Nb	69.6	59.7	66.1	69.6	63.9	57.5	55.2	64.2	61.5	44.2	47.1	43.4	48.0	39.8
Ba	567	485	571	765	488	479	501	571	573	457	500	481	395	340
La	48.1	40.0	45.1	50.1	47.8	42.5	33.0	42.8	41.0	31.5	32.7	31.4	34.9	29.1
Ce	104.9	76.3	91.5	101.5	103.3	83.9	33.0	42.8	41.0	67.3	65.8	63.1	69.8	58.4
Nd	47.3	40.5	44.0	39.2	43.4	41.7	34.4	42.8	39.8	30.8	29.6	27.0	36.1	30.3
Sm	9.10	8.10	8.97	7.92	7.89	8.72	7.69	8.54	8.52	6.64	6.90	6.86	8.02	7.08
Eu	3.30	2.60	2.95	2.78	2.78	2.94	2.56	2.86	2.90	2.43	2.37	2.27	2.65	2.34
Tb	0.91	0.76	0.74	0.77	0.88	0.87	0.75	0.77	0.73	0.79	0.62	0.62	0.84	0.77
Yb	1.69	1.51	1.35	1.82	1.80	1.67	1.11	1.41	1.45	1.59	1.31	1.35	1.66	1.54
Lu	0.18	0.19	0.21	0.23	0.29	0.23	0.16	0.21	0.20	0.23	0.24	0.25	0.21	0.22
Hf	7.75	6.10	6.39	6.01	6.75	5.85	5.55	6.43	6.56	5.74	5.18	5.13	5.33	4.80
Ta	5.43	4.10	4.69	4.89	4.98	3.86	3.65	4.94	4.61	3.19	2.92	2.72	5.04	2.45
Th	5.76	4.16	6.01	6.18	5.81	5.28	4.42	5.52	5.44	4.23	4.61	4.56	4.63	4.00
U	1.38	1.17	1.38	0.95	1.47	1.50	1.08	1.38	1.30	0.66	1.09	1.25	1.30	1.09
$[La/Sm]_N$	3.42	3.19	3.25	4.09	3.92	3.15	2.77	3.24	3.11	3.07	3.06	2.96	2.81	2.66
$[Nb/Th]_N$	1.42	1.69	1.29	1.32	1.29	1.28	1.47	1.37	1.33	1.23	1.20	1.12	1.22	1.17
$[Ta/U]_N$	2.02	1.79	1.74	2.64	1.74	1.32	1.73	1.83	1.82	2.48	1.37	1.11	1.99	1.15
Nb/U	50.43	51.03	47.90	73.26	43.47	38.32	51.11	46.52	47.31	66.97	43.21	34.72	36.92	36.51
Zr/Hf	42.89	47.13	48.29	41.63	41.08	42.60	46.36	46.31	43.84	38.59	45.12	43.86	45.29	42.92
Sr-Nd-Pb isotopes														
$^{87}Sr/^{86}Sr$	0.703833				0.704170		0.703537	0.703544	0.703571			0.704017	0.704019	
$^{143}Nd/^{144}Nd$	0.512891				0.512874		0.512876	0.512897	0.512881			0.512885	0.512912	
$^{206}Pb/^{204}Pb$					18.661		18.645	18.621	18.615			18.646		
$^{207}Pb/^{204}Pb$					15.610		15.536	15.519	15.505			15.607		
$^{208}Pb/^{204}Pb$					38.87		38.71	38.67	38.64			38.89		

Supplementary Table 3 Continued

Locality	Hainan Island (Tu et al., 1991 & Flower et al., 1992)													
Sample	HN55	HN57	HN69	HN87	HN22	HN76	HN77	HN23	HN35	HN36	HN37	HN41	HN95	HN96
Rock Type	OT	OT	OT	OT	OT	OT	OT	OT	OT	OT	OT	OT	OT	OT
Major elements (wt. %)														
SiO_2	49.48	49.86	50.01	50.41	49.89	50.79	50.20	52.59	52.17	52.86	52.40	52.53	52.20	52.66
TiO_2	2.24	2.23	2.29	2.31	2.44	2.33	2.31	2.19	2.16	2.23	2.22	2.01	2.03	2.14
$A1_2O_3$	14.11	14.24	14.50	14.54	15.01	14.68	14.58	14.85	14.84	15.27	15.50	14.62	14.44	14.68
TFe_2O_3	11.37	11.30	12.07	11.81	11.40	12.02	11.88	11.14	11.00	11.58	11.48	10.83	11.76	11.66
MnO	0.15	0.14	0.15	0.15	0.14	0.15	0.15	0.14	0.14	0.14	0.14	0.14	0.14	0.15
MgO	7.96	7.95	6.94	7.74	6.53	6.94	7.13	6.33	6.77	6.35	5.87	7.15	6.91	6.95
CaO	8.46	8.25	8.62	8.57	9.15	8.65	8.58	8.96	9.08	8.53	8.40	8.61	8.40	8.38
Na_2O	3.09	3.07	3.46	3.46	3.04	3.53	3.51	3.29	3.27	3.25	3.30	3.09	3.07	3.23
K_2O	1.66	1.62	1.60	1.59	1.46	1.62	1.71	1.43	1.35	1.37	1.37	1.51	1.41	1.46
P_2O_5	0.47	0.52	0.50	0.49	0.43	0.53	0.51	0.42	0.37	0.37	0.37	0.38	0.33	0.32
Total	98.99	99.18	100.15	101.08	99.49	101.26	100.56	101.34	101.15	101.96	101.05	100.86	100.71	101.64
Mg#	61.8	61.9	57.0	60.3	57.1	57.2	58.2	56.8	58.6	55.8	54.2	60.3	57.5	57.8
Trace elements (ppm)														
Sc	19.9	17.4	22.2	21.3	24.5	24.1	21.0	18.9	22.4	19.9	21.2	24.1	16.0	20.9
V	165	162	237	159	196	193	173	170	195	162	168	173	148	151
Cr	217	212	227	233	263	230	224	230	269	136	102	278	204	199
Co	64.4	52.5	60.2	53.9	49.7	56.3	52.1	51.2	56.6	62.6	60.1	56.1	57.4	62.2
Ni	159	165	152	172	87	159	173	84	95	135	122	126	158	157
Cu	51.5	52.9	58.0	66.8	52.6	52.6	55.0	67.2	54.2	53.7	55.4	51.0	54.1	56.3
Zn	120	112	126	118	119	125	118	113	113	122	118	113	124	131
Rb	28.0	32.3	35.1	33.9	22.6	29.1	36.8	26.5	27.5	25.3	26.0	30.7	29.7	29.0
Sr	513	487	554	547	554	579	552	456	476	446	455	446	438	442
Y	24.0	23.1	26.2	25.5	25.2	27.1	25.7	22.6	23.5	24.3	24.9	22.7	22.9	23.8
Zr	199	191	200	201	213	211	200	176	179	170	171	160	164	169
Nb	36.1	35.3	37.3	37.6	34.6	38.7	37.9	28.5	27.9	25.6	25.1	28.4	25.6	27.0
Ba	348	350	338	322	376	320	319	274	262	225	227	296	259	272
La	27.4	25.2	26.2	26.5	24.6	26.8	26.9	20.1	20.2	16.4	16.3	20.5	18.0	18.8
Ce	55.9	50.6	52.9	52.8	54.3	53.7	53.9	44.2	43.5	33.9	34.7	40.5	37.7	40.2
Nd	28.9	26.2	30.2	31.2	27.5	29.8	28.3	22.8	21.6	21.2	19.1	20.7	18.6	19.6
Sm	6.63	5.95	6.83	6.49	6.10	6.73	6.64	5.69	5.55	5.25	5.31	5.54	5.00	5.23
Eu	2.23	1.99	2.33	2.30	2.29	2.34	2.36	1.92	1.90	1.85	1.87	1.92	1.73	1.81
Tb	0.80	0.66	0.80	0.79	0.81	0.84	0.83	0.66	0.67	0.69	0.65	0.66	0.56	0.62
Yb	1.67	1.36	1.62	1.56	1.47	1.44	1.65	1.43	1.44	1.41	1.57	1.56	1.30	1.50
Lu	0.21	0.19	0.24	0.19	0.21	0.24	0.20	0.24	0.20	0.22	0.20	0.21	0.19	0.18
Hf	4.62	4.11	4.51	4.63	5.30	4.57	4.79	4.05	3.92	3.81	3.72	3.88	3.57	3.51
Ta	2.30	2.23	2.16	2.14	2.37	2.34	2.33	1.98	1.75	1.56	1.59	1.55	1.49	1.64
Th	3.80	3.63	3.11	3.22	3.29	3.21	3.36	2.93	2.88	2.27	2.31	2.95	2.90	2.83
U	0.98	0.68	0.87	0.81	1.04	0.95	1.06	0.79	0.84	0.72	0.75	0.85	0.67	0.81
$[La/Sm]_N$	2.67	2.74	2.48	2.64	2.61	2.57	2.62	2.29	2.35	2.02	1.98	2.39	2.33	2.32
$[Nb/Th]_N$	1.12	1.14	1.41	1.37	1.24	1.42	1.33	1.14	1.14	1.33	1.28	1.13	1.04	1.12
$[Ta/U]_N$	1.20	1.68	1.27	1.35	1.17	1.26	1.13	1.28	1.07	1.11	1.09	0.93	1.14	1.04
Nb/U	36.84	51.91	42.87	46.42	33.27	40.74	35.75	36.08	33.21	35.56	33.47	33.41	38.21	33.33
Zr/Hf	43.12	46.35	44.30	43.30	40.09	46.24	41.82	43.48	45.71	44.72	45.83	41.26	46.05	48.12
Sr-Nd-Pb isotopes														
$^{87}Sr/^{86}Sr$	0.704190				0.703824	0.703833	0.703814			0.704032		0.703985	0.704178	
$^{143}Nd/^{144}Nd$	0.512868				0.512866	0.512930	0.512926			0.512871		0.512819	0.512866	
$^{206}Pb/^{204}Pb$	18.674				18.464	18.636	18.660			18.667		18.720	18.667	
$^{207}Pb/^{204}Pb$	15.612				15.614	15.581	15.613			15.601		15.649	15.619	
$^{208}Pb/^{204}Pb$	38.98				38.88	38.79	38.88			38.85		38.98	38.99	

Supplementary Table 3 Continued

Locality	Hainan Island (Tu et al., 1991 & Flower et al., 1992)													
Sample	HN83	HN40	HN68	HN75	HN90	HN5	HN6	HN8	HN34	HN91	HN10	HN13	HN17	HN19
Rock Type	OT	OT	OT	OT	OT	QT	QT	QT	QT	QT	QT	QT	QT	QT
Major elements (wt. %)														
SiO_2	51.93	52.26	52.89	52.28	52.88	54.77	53.55	54.24	52.20	52.56	51.22	52.12	52.21	49.10
TiO_2	2.18	2.14	1.96	1.96	1.91	1.99	1.81	1.60	1.77	1.84	1.95	1.75	1.77	1.87
$A1_2O_3$	14.63	15.13	14.14	14.75	14.44	14.42	14.27	14.83	14.66	14.35	14.06	14.23	14.16	14.63
TFe_2O_3	11.50	11.42	11.29	11.76	11.15	11.60	11.67	11.69	12.09	10.99	11.40	11.24	11.15	9.57
MnO	0.14	0.14	0.14	0.14	0.14	0.15	0.17	0.14	0.15	0.13	0.15	0.16	0.14	0.29
MgO	7.29	6.53	7.06	6.94	7.39	6.82	8.07	6.95	7.11	6.81	6.94	7.27	6.70	5.41
CaO	8.51	8.47	8.49	8.30	8.36	8.44	8.58	8.67	8.59	8.32	8.57	8.62	8.13	12.45
Na_2O	3.38	3.34	2.90	3.08	3.03	3.09	3.00	3.04	2.89	3.01	2.80	2.99	2.89	2.88
K_2O	1.41	1.24	1.12	1.02	1.16	0.91	0.78	0.93	0.83	0.93	0.61	0.70	0.72	0.53
P_2O_5	0.42	0.36	0.32	0.33	0.29	0.23	0.25	0.25	0.23	0.26	0.28	0.24	0.25	0.28
Total	101.40	101.03	100.32	100.55	100.76	102.42	102.16	102.35	100.51	99.21	97.98	99.32	98.13	97.02
Mg#	59.4	56.8	59.1	57.7	60.3	57.6	61.4	57.7	57.5	58.8	58.4	60.1	58.2	56.6
Trace elements (ppm)														
Sc	21.8	20.2	18.3	20.9	22.6	23.4	20.9	21.1	25.1	21.8	19.5	25.0	20.3	25.5
V	161	155	163	163	144	138	141	138	165	152	147	140	128	149
Cr	224	146	297	243	230	215	291	208	218	207	193	248	254	237
Co	52.3	60.1	57.1	54.8	67.5	57.2	66.6	58.6	59.1	54.5	61.6	61.8	48.5	64.7
Ni	151	136	146	173	172	172	230	137	158	181	184	170	168	150
Cu	55.6	44.1	57.7	63.9	58.1	68.5	75.0	59.6	67.2	66.1	68.5	52.7	70.4	70.3
Zn	113	117	123	130	118	118	118	116	123	119	120	112	110	124
Rb	28.0	22.0	23.9	20.1	19.4	19.8	17.4	23.5	16.0	17.1	11.3	14.7	13.0	10.6
Sr	498	442	375	401	367	337	329	311	306	337	365	319	322	346
Y	23.9	24.4	22.4	24.2	21.3	22.8	21.5	20.2	21.2	22.4	20.7	21.6	22.2	23.0
Zr	182	164	146	152	143	150	120	120	121	134	130	112	117	126
Nb	31.2	23.1	20.7	24.4	20.4	22.2	21.1	16.8	16.9	18.7	19.0	18.7	18.9	21.1
Ba	272	214	153	160	127	148	186	169	127	124	135	168	186	216
La	22.2	16.2	15.0	17.5	15.1	12.8	13.5	13.0	11.8	12.3	12.7	13.0	12.9	15.4
Ce	42.9	33.5	31.3	34.8	32.3	28.2	26.9	27.5	25.3	26.8	25.5	27.3	30.1	32.7
Nd	20.8	17.9	17.3	20.4	18.2	15.5	14.4	14.5	14.1	12.6	15.2	13.5	16.8	16.3
Sm	5.99	5.06	4.78	5.36	4.77	4.10	4.15	3.84	3.83	4.47	4.24	3.79	4.00	4.40
Eu	2.04	1.84	1.76	1.93	1.78	1.71	1.51	1.46	1.39	1.61	1.63	1.53	1.60	1.75
Tb	0.79	0.59	0.72	0.79	0.67	0.70	0.79	0.57	0.85	0.69	0.73	0.62	0.69	0.73
Yb	1.23	1.44	1.50	1.61	1.41	1.77	1.38	1.57	1.50	1.17	1.56	1.75	1.66	1.50
Lu	0.18	0.21	0.18	0.21	0.22	0.20	0.19	0.19	0.22	0.17	0.18	0.19	0.18	0.21
Hf	4.13	4.10	3.40	3.89	3.62	4.20	2.71	3.16	2.67	3.04	3.65	3.17	3.36	3.58
Ta	1.91	1.38	1.17	1.31	1.35	1.60	1.42	1.11	0.85	1.12	1.42	1.03	1.16	1.30
Th	2.65	1.40	2.29	2.44	2.18	1.67	1.90	2.05	1.73	1.89	1.42	1.75	1.80	1.91
U	0.90	0.64	0.64	0.60	0.68	0.60	0.35	0.68	0.40	0.65	0.42	0.59	0.44	0.44
$[La/Sm]_N$	2.40	2.07	2.03	2.11	2.05	2.02	2.10	2.19	1.99	1.78	1.94	2.22	2.08	2.26
$[Nb/Th]_N$	1.38	1.94	1.06	1.18	1.10	1.56	1.31	0.96	1.15	1.16	1.57	1.26	1.23	1.30
$[Ta/U]_N$	1.09	1.10	0.94	1.12	1.02	1.37	2.08	0.84	1.09	0.88	1.73	0.89	1.35	1.51
Nb/U	34.67	36.09	32.34	40.67	30.00	37.00	60.29	24.71	42.25	28.77	45.24	31.69	42.95	47.95
Zr/Hf	44.00	39.90	42.91	39.02	39.36	35.76	44.35	37.97	45.32	43.91	35.67	35.24	34.70	35.25
Sr-Nd-Pb isotopes														
$^{87}Sr/^{86}Sr$	0.703893	0.704028			0.704149					0.704308	0.704220			0.704474
$^{143}Nd/^{144}Nd$	0.512925	0.512907			0.512908					0.512881	0.512876			0.512859
$^{206}Pb/^{204}Pb$	18.593	18.682			18.679					18.738	18.726			18.622
$^{207}Pb/^{204}Pb$	15.542	15.619			15.568					15.611	15.603			15.597
$^{208}Pb/^{204}Pb$	38.69	38.91			38.78					38.90	38.84			38.82

Supplementary Table 3 Continued

Locality	Hainan Island (Flower et al., 1992)												
Sample	HN9	HN11	HN14	HN15	HN16	HN18	HN92	HN93	HN94	HN7	HN20	HN21	HN25
Rock Type	QT	QT	QT	QT	QT	QT	QT	QT	QT	QT	QT	OT	OT
Major elements (wt. %)													
SiO_2	54.08	52.34	53.20	51.59	51.85	51.25	52.42	52.09	51.71	53.65	51.72	50.67	51.22
TiO_2	1.59	2.02	1.86	1.89	1.81	1.83	1.81	1.81	1.73	2.06	2.36	2.41	2.41
$A1_2O_3$	14.82	14.52	14.54	14.25	14.21	14.41	14.16	14.21	14.40	14.11	14.53	14.88	14.85
TFe_2O_3	14.90	11.84	10.40	11.28	10.95	11.26	10.96	11.09	11.56	11.52	11.29	11.43	11.15
MnO	0.15	0.19	0.12	0.16	0.16	0.14	0.13	0.13	0.14	0.23	0.14	0.14	0.14
MgO	7.09	6.57	6.56	6.08	6.58	7.16	7.06	6.94	6.79	6.98	6.42	6.64	6.48
CaO	8.72	8.77	8.13	8.47	9.27	8.40	8.30	8.28	8.51	8.74	8.43	9.15	8.95
Na_2O	3.02	3.14	2.98	2.97	2.98	2.82	3.01	3.02	2.74	3.13	2.99	3.20	3.38
K_2O	0.89	0.97	0.72	1.05	0.67	0.59	0.92	0.94	0.61	0.94	1.56	1.59	1.69
P_2O_5	0.25	0.27	0.29	0.34	0.26	0.25	0.25	0.22	0.19	0.29	0.41	0.43	0.42
Total	105.51	100.64	98.80	98.09	98.73	98.11	99.02	98.74	98.38	101.66	99.86	100.55	100.70
Mg#	57.9	56.0	59.4	55.4	58.0	59.5	59.8	59.1	57.6	58.2	57.0	57.4	57.3
Trace elements (ppm)													
Sc	21.9	22.1	23.3	18.0	22.0	23.8	23.0	19.0	24.2	21.6	21.0	19.2	21.2
V	142	145	145	131	136	143	145	142	133	140	193	196	198
Cr	211	202	226	225	246	233	233	314	205	241	282	261	271
Co	66.4	58.5	45.5	55.7	52.6	51.9	53.0	50.5	48.9	61.4	59.6	52.9	56.0
Ni	144	165	173	155	161	171	176	170	135	184	87	88	87
Cu	61.2	67.8	90.8	94.7	66.1	66.9	64.7	65.5	50.0	83.2	37.6	52.5	49.3
Zn	111	125	107	125	112	116	116	113	120	114	118	117	120
Rb	21.4	19.3	15.4	22.3	13.4	9.2	16.5	18.9	11.8	20.9	34.4	25.6	27.7
Sr	214	380	318	330	341	322	329	330	336	320	517	549	525
Y	18.9	21.0	21.8	29.0	22.7	21.9	21.1	21.3	18.4	23.9	24.6	25.2	24.7
Zr	117	140	118	165	120	122	131	133	124	139	202	210	205
Nb	17.6	19.5	19.2	24.6	20.6	20.9	18.6	17.0	16.8	24.6	33.3	34.4	34.1
Ba	160	152	177	262	192	183	129	127	133	206	336	378	369

Locality	Hainan Island (Flower et al., 1992)												
Sample	HN26	HN29	HN30	HN31	HN38	HN39	HN42	HN44	HN45	HN46	HN47	HN48	HN49
Rock Type	OT	AB	OT	OT	OT	OT	OT	OT	OT	OT	OT	OT	OT
Major elements (wt. %)													
SiO_2	51.94	46.49	49.49	50.26	53.05	51.53	52.66	48.98	48.87	49.42	50.38	49.62	48.71
TiO_2	2.11	2.66	2.42	2.51	2.21	2.23	2.20	2.69	2.44	2.43	2.53	2.46	2.42
$A1_2O_3$	14.94	13.59	13.87	14.07	15.49	15.61	15.23	14.31	14.03	14.27	14.30	14.45	14.05
TFe_2O_3	11.08	13.11	11.43	11.24	11.38	11.58	11.17	11.58	11.30	11.06	11.22	11.15	11.51
MnO	0.15	0.18	0.14	0.14	0.14	0.14	0.14	0.15	0.15	0.14	0.14	0.14	0.15
MgO	6.80	9.12	8.10	7.49	6.14	6.03	5.81	7.58	7.18	6.95	7.31	7.35	8.00
CaO	8.57	10.23	9.24	9.25	8.61	8.59	8.47	9.59	9.08	9.06	9.27	9.24	8.60
Na_2O	3.18	2.48	3.12	3.36	3.45	3.28	3.26	2.97	2.86	3.02	3.30	3.01	2.97
K_2O	1.20	1.44	1.93	2.03	1.37	1.16	1.34	1.92	1.81	1.83	2.05	1.78	1.80
P_2O_5	0.38	0.63	0.47	0.52	0.35	0.35	0.37	0.65	0.56	0.55	0.52	0.55	0.55
Total	100.37	99.92	100.21	100.88	102.19	100.51	100.65	100.44	98.29	98.73	101.00	99.75	98.77
Mg#	58.6	61.7	62.1	60.5	55.4	54.6	54.5	60.2	59.5	59.2	60.0	60.4	61.6
Trace elements (ppm)													
Sc	23.4	24.5	20.0	20.2	19.6	21.2	20.8	23.2	18.4	17.2	22.1	17.1	18.4
V	154	246	193	199	161	170	162	175	161	171	172	178	163
Cr	258	271	502	283	123	132	117	189	233	371	426	210	233
Co	62.2	64.7	62.9	55.2	60.4	60.0	53.1	52.8	51.4	51.0	55.1	57.6	52.9
Ni	142	196	145	122	124	133	115	153	146	177	159	156	153
Cu	63.4	56.0	60.5	62.3	54.4	48.8	60.5	54.1	55.7	52.2	49.7	51.6	52.6
Zn	119	128	116	114	119	121	118	119	116	114	113	117	120
Rb	20.1	27.4	39.9	43.9	25.0	18.7	25.1	40.7	38.3	38.7	36.3	36.7	37.2
Sr	456	720	597	504	448	453	440	654	580	573	574	611	567
Y	24.3	29.9	23.7	26.1	23.9	23.4	25.1	27.6	25.5	27.3	25.9	26.2	25.7
Zr	181	278	214	222	172	166	165	242	218	216	218	224	222
Nb	27.0	64.2	40.4	43.7	25.2	25.1	24.6	48.6	41.9	40.0	41.7	44.6	42.6
Ba	266	534	452	450	234	235	226	419	385	388	383	409	376

Supplementary Table 3 Continued

Locality	Hainan Island (Flower et al., 1992)												
Sample	HN50	HN51	HN52	HN53	HN56	HN58	HN59	HN60	HN61	HN65	HN66	HN67	HN70
Rock Type	OT	OT	OT	OT	OT	OT	OT	OT	OT	OT	OT	OT	OT
Major elements (wt. %)													
SiO_2	49.10	48.82	49.50	49.03	53.05	48.36	48.96	49.10	48.55	53.11	48.82	49.50	49.03
TiO_2	2.41	2.40	2.44	2.37	2.27	2.31	2.33	2.41	2.39	2.00	2.40	2.44	2.37
$A1_2O_3$	14.17	13.98	14.34	13.95	14.42	13.72	14.03	14.04	13.94	14.54	13.98	14.34	13.95
TFe_2O_3	11.40	11.24	11.43	11.49	10.83	11.54	11.53	11.86	11.50	10.71	11.24	11.43	11.49
MnO	0.14	0.15	0.14	0.14	0.12	0.15	0.15	0.15	0.15	0.14	0.15	0.14	0.14
MgO	8.02	7.48	7.29	8.06	6.82	8.84	7.86	8.44	8.45	6.71	7.48	7.29	8.06
CaO	8.42	9.04	8.72	8.21	8.87	8.78	7.06	8.56	8.67	8.66	9.04	8.72	8.21
Na_2O	2.89	2.99	3.13	2.89	3.18	2.81	2.98	2.97	2.78	2.96	2.99	3.13	2.89
K_2O	1.80	1.77	1.87	1.84	1.68	1.65	1.72	1.75	1.77	1.22	1.77	1.87	1.84
P_2O_5	0.53	0.56	0.55	0.54	0.48	0.51	0.53	0.53	0.54	0.32	0.56	0.55	0.54
Total	98.88	98.43	99.41	98.52	101.73	98.67	97.16	99.82	98.75	100.38	98.43	99.41	98.52
Mg#	61.9	60.6	59.5	61.8	59.3	63.9	61.1	62.1	62.9	59.2	60.6	59.5	61.8
Trace elements (ppm)													
Sc	21.8	16.3	19.1	14.8	18.5	15.4	19.7	21.6	17.9	22.4	20.1	23.0	19.1
V	170	165	177	167	176	158	159	158	164	163	165	166	184
Cr	194	202	383	194	209	208	364	206	210	245	232	244	223
Co	49.4	54.2	55.5	53.9	50.9	53.7	54.0	50.7	52.2	51.9	52.5	51.4	54.3
Ni	150	149	159	163	162	185	171	169	173	129	142	133	147
Cu	53.6	53.2	52.6	54.3	51.3	51.9	50.8	53.1	51.7	47.0	45.1	52.1	61.6
Zn	115	114	122	120	119	110	113	113	113	109	113	112	118
Rb	39.8	36.4	35.0	36.6	34.8	34.4	36.2	36.7	38.7	25.0	24.9	25.8	21.0
Sr	579	561	547	528	516	547	565	558	811	407	397	394	469
Y	26.0	25.0	25.8	26.0	25.7	25.3	25.3	25.0	26.1	23.2	23.3	23.5	24.8
Zr	217	216	219	221	204	207	201	210	206	152	151	150	177
Nb	41.9	42.2	41.7	43.5	37.1	38.9	39.0	41.0	41.5	23.0	22.4	23.1	28.2
Ba	391	375	383	357	328	368	364	410	405	210	173	179	254

Locality	Hainan Island (Flower et al., 1992)												
Sample	HN71	HN72	HN73	HN74	HN78	HN79	HN80	HN81	HN82	HN84	HN85	HN86	HN88
Rock Type	OT	OT	OT	OT	OT	OT	OT	OT	OT	OT	OT	OT	OT
SiO_2	53.05	48.36	48.96	49.10	48.55	53.11	50.71	52.53	50.76	50.79	50.86	50.82	50.50
TiO_2	2.27	2.31	2.33	2.41	2.39	2.00	2.28	2.27	2.31	2.28	2.30	2.30	2.31
$A1_2O_3$	14.42	13.72	14.03	14.04	13.94	14.54	14.46	14.44	14.62	14.57	14.69	14.35	14.34
TFe_2O_3	10.83	11.54	11.53	11.86	11.50	10.71	11.74	11.73	11.76	11.64	11.60	11.84	11.72
MnO	0.12	0.15	0.15	0.15	0.15	0.14	0.15	0.15	0.15	0.15	0.15	0.14	0.15
MgO	6.82	8.84	7.86	8.44	8.45	6.71	7.62	7.53	7.60	7.63	7.54	7.83	7.62
CaO	8.87	8.78	7.06	8.56	8.67	8.66	8.64	8.58	8.59	8.56	8.62	8.53	8.58
Na_2O	3.18	2.81	2.98	2.97	2.78	2.96	3.48	3.45	3.49	3.43	3.52	3.52	3.44
K_2O	1.68	1.65	1.72	1.75	1.77	1.22	1.54	1.55	1.57	1.55	1.59	1.56	1.60
P_2O_5	0.48	0.51	0.53	0.53	0.54	0.32	0.48	0.47	0.49	0.45	0.50	0.47	0.51
Total	101.73	98.67	97.16	99.82	98.75	100.38	101.11	102.71	101.34	101.05	101.37	101.36	100.77
Mg#	59.3	63.9	61.1	62.1	62.9	59.2	60.0	59.8	59.9	60.2	60.0	60.4	60.1
Trace elements (ppm)													
Sc	25.6	18.2	23.2	18.9	21.9	18.1	15.9	19.6	22.3	23.6	23.7	19.6	22.7
V	162	152	156	151	162	160	159	157	160	156	164	161	164
Cr	236	198	209	211	233	274	606	231	228	228	216	229	232
Co	56.8	53.1	53.9	52.4	52.6	52.7	50.4	49.1	54.3	55.2	53.8	51.7	61.0
Ni	179	176	179	170	166	159	157	153	155	158	154	166	169
Cu	61.6	61.4	62.6	55.6	65.2	54.5	57.2	57.9	74.6	66.2	71.5	61.9	53.6
Zn	122	117	116	119	117	116	109	116	114	117	115	117	116
Rb	22.6	20.9	22.2	20.4	30.4	30.1	29.1	30.1	30.5	31.1	30.3	30.1	31.6
Sr	404	396	401	396	547	538	533	542	548	539	549	555	552
Y	23.3	23.0	24.4	21.6	25.2	25.4	24.4	25.6	25.9	26.4	25.4	26.6	25.0
Zr	157	152	155	152	199	196	193	197	203	198	201	200	199
Nb	23.1	22.6	22.9	22.5	36.7	36.4	34.1	35.3	36.1	34.8	35.7	35.7	37.2
Ba	167	167	170	178	326	296	301	296	329	302	340	312	318

Supplementary Table 3 Continued

Locality	Hainan Island (Zou & Fan, 2010)									
Sample	HN9901	HN9902	106B1	HN9907	HN9908	HN9910	HN9911	HN9912	HN9914	119B1
Rock Type	OT	OT	OT	OT	AOB	AOB	AOB	AOB	OT	QT
Major elements (wt. %)										
SiO_2	51.74	50.77	50.99	49.10	45.32	45.47	45.14	45.27	49.87	53.14
TiO_2	2.34	2.37	2.27	2.30	2.81	2.76	2.76	2.75	2.17	1.62
$A1_2O_3$	14.32	15.12	14.33	13.36	12.83	12.98	12.99	12.76	13.86	14.36
TFe_2O_3	10.64	10.42	10.97	11.42	12.79	12.67	11.52	12.63	10.41	10.07
MnO	0.15	0.25	0.14	0.27	0.20	0.31	0.19	0.20	0.15	0.14
MgO	6.53	6.81	7.47	9.63	10.29	10.17	9.90	10.29	9.08	6.80
CaO	8.92	9.24	9.28	9.46	10.57	10.80	10.43	10.46	9.37	8.53
Na_2O	3.41	2.82	2.71	2.55	2.85	2.42	2.95	3.12	3.12	3.03
K_2O	1.68	1.46	1.38	1.53	1.64	1.43	1.61	1.63	1.53	1.00
P_2O_5	0.47	0.47	0.47	0.48	0.86	0.82	0.75	0.79	0.42	0.23
Total	100.19	99.73	100.02	100.11	100.15	99.84	98.24	99.88	99.97	98.93
Mg#	59.0	60.0	61.0	66.0	65.0	65.0	66.0	65.0	67.0	61.0
Trace elements (ppm)										
Rb	35.6	30.0	28.8	32.4	36.5	35.0	35.2	38.8	30.0	23.6
Sr	546	559	489	557	817	820	769	811	525	318
Y	23.4	23.3	25.5	22.7	30.0	29.8	28.6	29.1	21.2	18.8
Zr	188	189	198	191	309	309	289	294	152	108
Nb	33.6	33.7	41.1	46.1	84.1	83.9	77.1	79.1	33.8	16.4
Ba	396	423	351	396	573	574	535	536	353	216
La	24.9	24.9	29.5	33.3	64.8	64.1	58.9	59.4	22.3	14.0
Ce	49.4	49.6	57.6	65.2	125.7	125.5	114.8	116.5	43.4	27.5
Pr	6.2	6.26	7.38	7.83	14.79	14.71	13.55	13.58	5.4	3.44
Nd	26.9	27.1	30.8	32.0	57.2	57.0	52.3	52.2	23.0	15.2
Sm	6.94	6.83	6.64	7.07	10.89	10.77	10.26	10.10	5.79	4.14
Eu	2.34	2.36	2.11	2.33	3.35	3.37	3.15	3.24	2.05	1.48
Gd	6.79	6.85	6.44	6.52	9.12	9.15	8.85	8.65	5.95	4.56
Tb	1.03	1.01	0.96	0.97	1.28	1.29	1.24	1.23	0.88	0.73
Dy	5.52	5.51	5.22	5.25	6.96	6.94	6.65	6.53	4.87	4.18
Ho	0.98	0.96	0.91	0.94	1.23	1.21	1.18	1.16	0.86	0.78
Er	2.26	2.20	2.19	2.23	2.97	2.87	2.77	2.72	2.07	1.89
Yb	1.61	1.53	1.78	1.66	2.17	2.15	2.04	2.06	1.46	1.44
Lu	0.22	0.22	0.26	0.24	0.32	0.32	0.30	0.31	0.22	0.21
Hf	4.85	4.92	4.80	4.87	7.60	7.72	7.24	7.16	3.93	3.02
Ta	2.04	2.04	2.44	2.80	5.20	5.25	4.77	4.79	2.05	0.98
Pb	3.03	3.53	4.06	3.53	5.19	5.27	3.98	4.84	2.48	2.79
Th	3.87	3.90	4.29	4.70	8.36	8.29	7.63	7.76	3.38	2.73
U	0.91	0.88	0.99	1.19	2.00	1.96	1.81	1.81	0.79	0.59
$[La/Sm]_N$	2.32	2.36	2.87	3.04	3.85	3.85	3.71	3.80	2.49	2.19
$[Nb/Th]_N$	1.02	1.02	1.13	1.15	1.18	1.19	1.19	1.20	1.17	0.71
$[Ta/U]_N$	1.15	1.19	1.26	1.21	1.33	1.37	1.35	1.36	1.33	0.85
Sr/Sr*	1.22	1.24	0.94	1.02	0.81	0.81	0.83	0.88	1.36	1.27
Nb/U	36.93	38.30	41.47	38.75	42.04	42.81	42.57	43.67	42.76	27.80
Zr/Hf	38.76	38.41	41.25	39.22	40.66	40.03	39.92	41.06	38.68	35.76
Pb/Ce	0.06	0.07	0.07	0.05	0.04	0.04	0.03	0.04	0.06	0.10
Sr-Nd-Pb isotopes										
$^{87}Sr/^{86}Sr$	0.703853	0.703919		0.70418	0.70423	0.704273		0.704182		
$^{143}Nd/^{144}Nd$	0.512868	0.512884		0.512848	0.512869	0.512861		0.512862		
$^{206}Pb/^{204}Pb$	18.631			18.655	18.692	18.696		18.705		
$^{207}Pb/^{204}Pb$	15.605			15.633	15.647	15.63		15.622		
$^{208}Pb/^{204}Pb$	38.846			38.874	38.881	38.872		38.853		

Supplementary Table 3 Continued

Locality	Hainan Island (Ho et al., 2000)									
Sample	HK04	HK11A	HK14	HK16	HK17	HK22	HK24A	HK25	HK27	HK28
Rock Type	AOB	AOB	AOB	OT	QT	OT	AOB	OT	QT	QT
Major elements (wt. %)										
SiO_2	48.15	47.84	47.54	51.28	52.90	51.45	47.92	49.58	50.75	52.52
TiO_2	2.28	2.26	3.13	1.89	1.59	1.94	2.27	2.02	1.98	1.74
$A1_2O_3$	12.75	13.28	13.88	14.77	14.48	14.04	13.76	13.83	13.56	14.64
TFe_2O_3	11.46	11.82	12.02	10.71	11.00	10.83	11.39	11.29	10.59	11.02
MnO	0.15	0.15	0.15	0.14	0.14	0.13	0.15	0.15	0.14	0.14
MgO	8.79	10.42	7.56	6.76	6.39	7.19	9.17	7.94	6.96	5.81
CaO	7.69	9.27	8.88	8.92	9.56	8.18	9.56	9.58	9.10	8.44
Na_2O	3.12	2.86	3.49	3.26	3.09	3.76	3.33	3.13	2.98	3.09
K_2O	2.25	1.78	1.97	1.18	0.55	1.71	1.65	1.32	1.07	0.71
P_2O_5	0.78	0.45	0.67	0.35	0.19	0.43	0.42	0.37	0.24	0.24
Total	99.24	100.12	99.28	99.77	99.89	99.66	99.64	99.21	99.28	99.38
L.O.I.	1.81	-	-	0.51	-	-	-	-	1.91	1.04
Mg#	65.5	68.6	60.9	61.0	59.0	62.2	66.6	63.5	62.0	56.6
Trace elements (ppm)										
Sc	15.5	17.6	16.9	17.4	20.2	16.0	21.8	21.2	20.9	21.3
V	120	155	171	127	129	126	183	165	149	142
Cr	323	285	191	203	176	197	231	247	213	140
Co	50.0	64.0	55.0	60.0	52.0	55.0	55.0	52.0	50.0	51.0
Ni	301	294	139	189	110	150	222	200	164	117
Cu	27.0	54.0	53.0	55.0	59.0	54.0	53.0	57.0	63.0	56.0
Zn	137	112	126	120	108	121	109	112	105	111
Rb	50.0	41.0	43.0	24.0	12.0	33.0	32.0	21.0	24.0	13.0
Sr	840	520	661	438	259	554	609	443	341	321
Y	17.9	24.9	29.1	21.2	18.8	20.0	23.1	21.9	21.2	20.8
Zr	279	179	254	141	99	188	192	161	134	128
Nb	72.6	41.4	55.6	26.5	11.9	49.0	49.0	29.8	24.8	17.9
Ba	546	407	573	250	93	457	379	277	217	171
La	41.5	27.6	34.8	17.3	6.6	28.8	27.0	18.8	12.7	11.3
Ce	81.6	53.4	63.9	33.6	17.2	49.2	49.0	36.7	26.7	24.9
Nd	46.1	31.9	41.5	21.0	11.3	28.1	29.5	22.1	15.5	15.1
Sm	8.90	6.60	9.00	5.00	3.40	6.00	6.20	5.10	4.10	4.10
Eu	2.71	2.06	2.85	1.68	1.25	2.07	2.05	1.79	1.52	1.47
Tb	0.96	0.84	1.04	0.72	0.61	0.77	0.79	0.75	0.67	0.65
Yb	1.69	1.52	1.65	1.48	1.45	1.28	1.58	1.56	1.55	1.54
Lu	0.26	0.23	0.24	0.22	0.21	0.19	0.22	0.23	0.22	0.23
Hf	6.26	4.42	5.74	3.44	2.61	4.22	4.08	3.46	3.06	2.91
Th	6.10	4.52	5.14	2.72	1.17	4.41	3.78	2.99	2.10	1.70
U	1.49	0.98	1.15	0.77	0.32	0.70	0.80	0.83	0.58	0.51
$[La/Sm]_N$	3.01	2.70	2.50	2.24	1.25	3.10	2.81	2.38	2.00	1.78
$[Nb/Th]_N$	1.40	1.08	1.27	1.15	1.20	1.31	1.52	1.17	1.39	1.24
Nb/U	48.72	42.24	48.35	34.42	37.19	70.00	61.25	35.90	42.76	35.10
Zr/Hf	44.57	40.50	44.25	40.99	37.93	44.55	47.06	46.53	43.79	43.99

Supplementary Table 3 Continued

Locality	Hainan Island (Wang et al., 2011)												
Sample	08HN-2A	08HN-2B	08HN-3	08HN-4A	08HN-4B	08HN-4C	08HN-4D	08HN-4G	08HN-5A	08HN-5B	08HN-5C	08HN-5D	08HN-5E
Rock Type	AB	AB	OT	QT	QT	QT	OT	OT	OT	OT	OT	OT	OT
Major elements (wt. %)													
SiO_2	47.50	47.80	47.30	52.10	52.00	52.00	50.50	52.00	51.20	51.10	51.00	50.90	51.10
TiO_2	2.98	2.85	2.70	1.98	1.91	2.12	1.83	2.02	1.91	1.99	1.96	1.99	1.98
$A1_2O_3$	13.00	13.20	12.70	13.80	13.60	14.00	12.90	13.90	13.70	13.90	14.00	13.90	13.90
TFe_2O_3	13.20	13.00	13.50	11.60	11.80	11.60	12.00	11.60	12.30	11.90	11.90	12.00	11.80
MnO	0.14	0.14	0.14	0.12	0.13	0.13	0.15	0.13	0.13	0.14	0.14	0.14	0.14
MgO	9.68	9.29	10.60	7.79	8.13	7.25	10.40	7.47	7.85	7.75	7.99	7.83	7.76
CaO	7.89	8.00	8.22	8.60	8.47	8.79	8.58	8.49	8.92	8.56	8.63	8.60	8.76
Na_2O	3.40	3.32	2.69	2.94	2.89	2.96	2.70	3.09	2.91	3.15	3.08	3.16	3.16
K_2O	1.52	1.64	1.59	0.81	0.82	0.85	0.64	0.95	0.73	1.11	1.01	1.11	1.07
P_2O_5	0.67	0.69	0.49	0.24	0.23	0.32	0.28	0.28	0.30	0.36	0.35	0.36	0.36
Total	99.98	99.93	99.93	99.98	99.97	100.01	99.98	99.93	99.95	99.95	100.05	99.99	100.03
L.O.I.	0.73	0.72	0.85	0.60	0.76	0.89	0.68	0.20	1.29	0.71	0.92	0.68	0.67
Mg#	61.7	61.1	63.3	59.7	60.2	57.8	65.6	58.5	58.4	58.9	59.6	59.0	59.1
Trace elements (ppm)													
Sc	17.9	16.8	20.0		20.4	21.4	21.0				20.8	20.1	20.9
V	156	144	159		142	154	142				150	154	175
Cr	284	248	314		273	207	386				214	196	209
Co	50.5	47.0	55.9		43.7	40.5	49.5				41.6	43.3	43.2
Ni	268	248	307		191	168	310				156	162	162
Cu	47.8	41.2	51.4		60.6	66.4	53.3				56.6	57.7	58.4
Zn	140	125	120		113	114	104				105	109	108
Rb	50.0	50.1	26.4		15.8	13.4	6.4				15.9	21.9	17.7
Sr	764	906	587		318	382	388				391	429	431
Y	23.0	23.2	20.3		17.1	19.9	16.6				19.0	20.5	20.2
Zr	264	260	189		106	138	115				126	138	135
Nb	61.2	58.8	41.7		18.1	27.0	23.9				29.6	31.2	31.0
Ba	626	870	424		185	221	231				284	339	335
La	39.7	40.3	26.7		12.4	18.0	17.4				21.0	22.7	22.6
Ce	81.8	82.0	55.1		25.6	36.3	34.6				41.6	45.2	45.0
Pr	10.2	10.2	7.11		3.27	4.5	4.22				5	5.43	5.49
Nd	41.0	41.2	29.7		14.2	19.1	17.2				20.2	22.1	21.7
Sm	8.76	8.62	6.72		3.86	4.71	4.08				4.80	5.12	4.96
Eu	2.87	2.85	2.26		1.44	1.75	1.52				1.70	1.78	1.70
Gd	7.94	7.57	6.35		4.25	5.13	4.33				5.15	5.29	5.25
Tb	1.10	1.05	0.90		0.69	0.77	0.68				0.83	0.82	0.83
Dy	5.52	5.40	4.49		3.83	4.11	3.68				4.38	4.44	4.46
Ho	0.93	0.90	0.78		0.69	0.74	0.65				0.76	0.82	0.80
Er	2.22	2.12	1.86		1.78	1.86	1.58				1.96	2.01	1.97
Tm	0.27	0.27	0.24		0.22	0.24	0.21				0.26	0.26	0.27
Yb	1.53	1.56	1.42		1.31	1.39	1.23				1.49	1.51	1.53
Lu	0.21	0.22	0.21		0.19	0.20	0.18				0.21	0.22	0.22
Hf	6.23	6.25	4.55		2.76	3.41	2.96				3.25	3.34	3.33
Ta	4.18	3.98	2.81		1.13	1.57	1.50				1.84	1.74	1.80
Pb	2.69	2.40	1.88		5.45	1.34	1.57				1.61	4.43	2.43
Th	5.20	5.20	3.65		1.85	2.80	2.61				3.51	3.04	3.39
U	1.26	1.28	0.90		0.43	0.59	0.57				0.74	0.65	0.69
$[La/Sm]_N$	2.93	3.02	2.57		2.08	2.47	2.76				2.87	2.83	2.94
$[Nb/Th]_N$	1.38	1.33	1.34		1.15	1.13	1.08				1.05	1.14	1.08
$[Ta/U]_N$	1.70	1.59	1.61		1.36	1.35	1.34				1.38	1.27	1.33
Sr/Sr*	1.08	1.27	1.17		1.35	1.19	1.31				1.12	1.13	1.14
Nb/U	48.57	45.94	46.59		42.49	45.45	41.78				45.75	42.16	44.67
Zr/Hf	42.38	41.60	41.54		38.41	40.47	38.85				38.77	41.32	40.54
Pb/Ce	0.03	0.03	0.03		0.21	0.04	0.05				0.11	0.04	0.05

Supplementary Table 3 Continued

Locality	Hainan Island (Wang et al., 2011)												
Sample	08HN-5F	08HN-5G	08HN-5H	08HN-5I	08HN-5J	08HN-5K	08HN-6A	08HN-6B	08HN-6C	08HN-6D	08HN-6F	08HN-7A	08HN-7B
Rock Type	QT	OT	OT	QT	OT	OT	QT	QT	QT	QT	QT	QT	QT
Major elements (wt. %)													
SiO_2	52.10	51.20	51.00	51.50	51.00	51.10	53.20	52.90	52.90	53.30	52.90	52.80	53.10
TiO_2	1.93	2.00	1.97	1.96	1.89	2.22	1.81	1.78	1.80	1.84	1.78	1.77	1.66
$A1_2O_3$	13.90	13.90	14.00	13.90	13.90	13.90	14.40	14.30	14.40	14.50	14.20	14.50	14.50
TFe_2O_3	11.80	11.80	11.90	12.10	12.00	12.70	12.30	12.40	12.30	12.00	12.70	12.60	12.00
MnO	0.14	0.14	0.13	0.14	0.15	0.13	0.12	0.14	0.14	0.12	0.13	0.13	0.13
MgO	7.36	7.61	7.81	7.56	8.63	6.86	5.91	5.84	5.94	5.93	5.94	5.86	6.26
CaO	8.63	8.63	8.55	8.77	8.44	8.40	8.36	8.63	8.62	8.24	8.43	8.53	8.71
Na_2O	3.03	3.20	3.15	2.96	2.88	3.19	3.06	2.88	2.87	3.04	3.00	3.17	2.96
K_2O	0.80	1.11	1.10	0.75	0.86	1.09	0.69	0.83	0.81	0.72	0.67	0.51	0.46
P_2O_5	0.28	0.37	0.36	0.31	0.33	0.35	0.23	0.22	0.22	0.23	0.23	0.19	0.16
Total	99.96	99.95	99.97	99.94	100.07	99.95	100.08	99.93	100.00	99.92	99.97	100.06	99.93
L.O.I.	0.98	0.71	1.02	0.74	2.03	0.01	0.53	0.79	0.67	0.80	0.71	0.49	0.17
Mg#	57.8	58.7	59.0	57.9	61.4	54.3	51.4	50.8	51.5	52.1	50.7	50.6	53.4
Trace elements (ppm)													
Sc	20.9			22.3	20.5	22.0	20.3		21.4	20.2			22.2
V	146			152	140	161	141		144	136			142
Cr	200			196	214	171	138		150	154			167
Co	41.9			40.2	45.0	41.5	38.9		41.0	39.4			41.6
Ni	152			145	176	134	95		99	97			100
Cu	64.3			60.6	59.6	65.0	53.4		55.6	40.4			51.9
Zn	109			109	108	123	111		112	116			109
Rb	12.1			14.3	11.6	23.5	9.0		12.4	9.9			6.4
Sr	350			387	380	367	310		327	325			268
Y	19.7			20.3	19.4	22.1	17.0		16.6	17.3			17.4
Zr	116			124	125	146	111		110	117			91
Nb	20.7			25.0	28.5	28.6	14.6		14.6	15.7			9.7
Ba	205			228	292	239	145		136	151			82
La	15.7			18.0	20.4	20.1	11.3		11.3	11.7			8.2
Ce	31.8			36.4	40.8	40.8	24.2		24.7	25.7			17.6
Pr	3.98			4.59	4.98	5.12	3.23		3.3	3.36			2.56
Nd	16.9			18.4	20.3	21.3	14.4		14.5	14.6			12.2
Sm	4.46			4.57	4.77	5.07	3.97		3.97	4.04			3.56
Eu	1.57			1.68	1.64	1.70	1.46		1.48	1.53			1.36
Gd	4.81			5.05	4.87	5.49	4.32		4.27	4.43			4.1
Tb	0.78			0.80	0.77	0.89	0.72		0.71	0.70			0.68
Dy	4.27			4.30	4.16	4.74	3.91		3.79	3.75			3.81
Ho	0.78			0.77	0.77	0.87	0.72		0.69	0.67			0.71
Er	1.92			1.96	1.90	2.14	1.79		1.73	1.62			1.77
Tm	0.26			0.27	0.25	0.28	0.24		0.23	0.23			0.23
Yb	1.50			1.54	1.52	1.70	1.39		1.33	1.29			1.38
Lu	0.22			0.22	0.23	0.24	0.21		0.19	0.20			0.20
Hf	3.21			3.17	3.27	3.82	3.08		2.93	3.04			2.56
Ta	1.28			1.50	1.70	1.80	0.96		0.91	0.93			0.61
Pb	1.56			1.57	1.54	2.22	1.26		1.51	1.69			1.24
Th	2.38			2.78	3.15	3.13	1.55		1.54	1.60			0.98
U	0.51			0.57	0.63	0.66	0.35		0.38	0.37			0.23
$[La/Sm]_N$	2.28			2.55	2.76	2.56	1.84		1.84	1.87			1.49
$[Nb/Th]_N$	1.02			1.06	1.06	1.07	1.11		1.11	1.15			1.16
$[Ta/U]_N$	1.30			1.35	1.38	1.40	1.40		1.24	1.29			1.39
Sr/Sr*	1.23			1.21	1.09	1.01	1.32		1.37	1.34			1.39
Nb/U	40.99			43.86	45.02	43.53	41.60		38.83	42.43			43.07
Zr/Hf	36.14			39.12	38.23	38.22	36.04		37.54	38.49			35.39
Pb/Ce	0.05			0.04	0.04	0.05	0.05		0.06	0.07			0.07

Supplementary Table 3 Continued

Locality	Hainan Island (Wang et al., 2011)												
Sample	08HN-7D	08HN-7E	08HN-8A	08HN-8B	08HN-9A	08HN-9B	08HN-9C	08HN-10A	08HN-10B	08HN-10C	08HN-11A	08HN-11B	08HN-12A
Rock Type	QT	QT	OT	AB	QT	QT	QT	QT	QT	QT	QT	QT	OT
Major elements (wt. %)													
SiO_2	53.30	53.20	49.60	49.90	52.50	52.90	52.90	52.20	52.80	52.80	52.70	52.80	51.10
TiO_2	1.64	1.66	2.25	2.36	1.71	1.74	1.75	1.92	1.91	1.96	1.98	1.99	1.90
$A1_2O_3$	14.50	14.50	12.80	13.40	14.30	14.50	14.50	13.50	13.70	13.90	13.80	13.90	14.00
TFe_2O_3	11.90	12.10	12.70	12.30	13.20	12.70	11.80	11.70	11.80	11.40	11.40	11.20	11.30
MnO	0.13	0.13	0.17	0.13	0.13	0.13	0.13	0.12	0.13	0.13	0.13	0.12	0.10
MgO	6.18	6.43	8.96	7.61	5.97	6.05	6.00	7.05	7.19	7.15	6.77	6.78	7.09
CaO	8.69	8.36	8.31	8.61	8.66	8.38	8.73	9.27	8.26	8.40	9.04	8.97	8.88
Na_2O	2.94	2.90	3.24	3.47	2.91	2.89	3.41	2.97	3.00	3.08	2.88	2.90	3.56
K_2O	0.53	0.52	1.50	1.71	0.45	0.50	0.58	0.71	0.91	0.97	1.10	1.11	1.63
P_2O_5	0.16	0.17	0.44	0.48	0.17	0.18	0.18	0.26	0.26	0.26	0.27	0.27	0.39
Total	99.97	99.97	99.97	99.97	100.01	99.97	99.97	99.70	99.96	100.05	100.07	100.04	99.95
L.O.I.	0.01	0.21	-0.18	0.18	0.27	0.23	0.20	0.87	0.02	-0.16	0.53	0.34	1.61
Mg#	53.3	53.8	60.8	57.6	49.8	51.1	52.7	57.0	57.3	58.0	56.7	57.2	58.0
Trace elements (ppm)													
Sc		21.3	22.1			21.0		20.0	19.4		19.6		16.6
V		133	170			140		144	151		145		131
Cr		170	248			159		206	217		204		202
Co		43.2	58.7			42.9		42.0	41.7		41.0		44.1
Ni		102	165			111		156	156		138		144
Cu		51.0	47.9			45.0		55.8	57.2		53.3		54.9
Zn		107	128			111		111	111		106		118
Rb		7.1	22.0			7.2		13.9	13.9		17.2		20.2
Sr		209	558			198		433	348		373		525
Y		16.4	21.3			44.6		19.5	18.8		19.4		16.3
Zr		90	199			94		122	122		128		170
Nb		10.1	37.3			11.3		15.6	15.9		16.6		39.6
Ba		94	524			114		146	143		159		443
La		8.4	25.4			37.3		12.4	12.3		12.6		25.2
Ce		18.5	50.7			82.2		27.5	27.0		27.6		48.7
Pr		2.71	6.4			10.9		3.66	3.59		3.7		5.9
Nd		12.7	27.1			45.5		16.3	16.0		16.4		23.7
Sm		3.71	6.40			11.70		4.55	4.40		4.36		5.48
Eu		1.44	2.26			4.18		1.63	1.59		1.60		2.00
Gd		4.15	6.35			11.6		4.79	4.74		4.71		5.56
Tb		0.68	0.90			1.93		0.76	0.75		0.78		0.81
Dy		3.72	4.61			9.99		4.23	4.11		4.22		3.89
Ho		0.70	0.80			1.75		0.77	0.77		0.75		0.63
Er		1.72	1.86			4.12		1.88	1.93		1.88		1.46
Tm		0.23	0.23			0.56		0.26	0.26		0.25		0.18
Yb		1.34	1.36			3.12		1.45	1.47		1.48		1.02
Lu		0.20	0.19			0.43		0.21	0.21		0.21		0.14
Hf		2.54	4.98			2.64		3.17	3.32		3.46		4.08
Ta		0.63	2.24			0.71		0.96	1.01		1.04		2.44
Pb		0.89	0.32			1.17		2.08	2.20		2.05		2.09
Th		1.04	3.32			1.06		1.98	2.02		2.21		4.13
U		0.26	0.86			0.32		0.48	0.48		0.53		0.29
$[La/Sm]_N$		1.47	2.56			2.06		1.76	1.81		1.87		2.97
$[Nb/Th]_N$		1.14	1.32			1.25		0.93	0.93		0.88		1.13
$[Ta/U]_N$		1.24	1.33			1.13		1.02	1.08		1.01		4.29
Sr/Sr*		1.03	1.22			0.26		1.62	1.33		1.39		1.28
Nb/U		38.85	43.22			34.88		32.43	33.13		31.32		136.08
Zr/Hf		35.59	39.96			35.61		38.49	36.75		36.99		41.67
Pb/Ce		0.05	0.01			0.01		0.08	0.08		0.07		0.04

Supplementary Table 3 Continued

Locality	Hainan Island (Wang et al., 2011)												
Sample	08HN-12B	08HN-13A	08HN-13B	08HN-14A	08HN-14B	08HN-15A	08HN-15B	08HN-16A	08HN-16B	08HN-16C	08HN-17A	08HN-17B	08HN-18A
Rock Type	OT	OT	OT	OT	OT	QT	QT	AB	AB	AB	OT	AB	QT
Major elements (wt. %)													
SiO_2	51.10	51.60	51.70	53.90	53.80	52.80	52.90	51.40	51.30	51.40	55.70	55.50	52.80
TiO_2	1.96	1.67	1.67	1.71	1.71	1.65	1.59	2.06	2.09	2.04	1.54	1.53	1.63
$A1_2O_3$	13.90	14.40	14.40	14.80	14.60	14.30	14.30	14.20	14.20	14.10	15.00	14.90	14.20
TFe_2O_3	11.90	11.70	11.80	10.40	10.40	12.30	12.30	11.30	11.40	11.30	9.10	9.04	12.50
MnO	0.12	0.12	0.13	0.10	0.10	0.13	0.13	0.11	0.11	0.11	0.09	0.09	0.13
MgO	7.32	7.09	6.98	5.54	5.83	6.66	6.64	6.69	6.80	6.79	4.89	4.96	6.56
CaO	7.79	8.19	8.10	6.01	6.20	8.43	8.50	6.86	7.03	6.94	4.90	4.86	8.48
Na_2O	3.73	3.56	3.56	4.52	4.45	3.01	2.99	4.30	4.10	4.28	4.89	5.11	2.96
K_2O	1.68	1.36	1.35	2.65	2.59	0.58	0.58	2.62	2.55	2.59	3.46	3.46	0.56
P_2O_5	0.39	0.29	0.29	0.44	0.43	0.17	0.16	0.48	0.48	0.47	0.49	0.47	0.18
Total	99.89	99.99	99.98	100.07	100.11	100.04	100.10	100.02	100.07	100.03	100.06	99.92	100.00
L.O.I.	-0.62	-0.17	-0.01	-0.28	-0.47	-0.32	-0.41	-0.46	-0.26	-0.54	0.20	-0.01	0.52
Mg#	57.4	57.2	56.5	54.0	55.3	54.4	54.4	56.7	56.8	57.1	54.2	54.7	53.6
Trace elements (ppm)													
Sc		18.8		12.9		21.7		18.4		14.6		9.5	
V		128		100		143		133		135		86	
Cr		267		178		190		173		171		116	
Co		46.0		35.8		45.5		41.5		39.5		29.1	
Ni		166		116		130		144		103		84	
Cu		52.6		33.1		62.0		55.5		48.6		42.3	
Zn		118		140		114		128		144		152	
Rb		20.0		35.3		8.4		17.4		39.2		56.5	
Sr		532		672		293		416		680		742	
Y		15.1		14.6		16.1		18.8		16.1		14.1	
Zr		135		291		94		148		275		440	
Nb		31.1		57.8		11.2		26.7		55.6		79.8	
Ba		365		644		106		218		533		711	
La		19.2		39.6		8.2		17.9		33.5		49.6	
Ce		38.5		73.8		18.3		37.4		66.6		92.6	
Pr		4.8		9.24		2.5		4.8		7.99		10.6	
Nd		19.3		36.0		11.8		20.9		31.3		38.7	
Sm		4.65		7.67		3.54		5.14		6.75		7.88	
Eu		1.62		2.62		1.34		1.77		2.28		2.57	
Gd		4.45		6.89		3.9		5.14		5.99		6.78	
Tb		0.68		0.92		0.64		0.82		0.84		0.90	
Dy		3.43		4.08		3.45		4.18		3.98		3.84	
Ho		0.57		0.60		0.65		0.76		0.61		0.55	
Er		1.38		1.30		1.66		1.78		1.39		1.09	
Tm		0.17		0.16		0.22		0.23		0.17		0.12	
Yb		0.99		0.79		1.24		1.34		0.95		0.68	
Lu		0.14		0.11		0.19		0.20		0.13		0.09	
Hf		3.51		6.97		2.57		3.70		6.48		9.69	
Ta		1.85		3.77		0.71		1.68		3.60		5.47	
Pb		1.27		3.37		1.26		2.37		2.91		4.36	
Th		2.95		5.88		1.18		2.77		5.44		8.63	
U		0.44		0.66		0.27		0.68		1.31		1.53	
$[La/Sm]_N$		2.67		3.34		1.50		2.25		3.21		4.07	
$[Nb/Th]_N$		1.24		1.16		1.12		1.13		1.20		1.09	
$[Ta/U]_N$		2.15		2.92		1.36		1.27		1.41		1.83	
Sr/Sr*		1.59		1.06		1.56		1.20		1.24		1.05	
Nb/U		70.52		87.44		41.95		39.32		42.44		52.16	
Zr/Hf		38.46		41.75		36.50		40.00		42.44		45.41	
Pb/Ce		0.03		0.05		0.07		0.06		0.04		0.05	

Supplementary Table 3 Continued

Locality	Hainan Island (Wang et al., 2011)												
Sample	08HN-18B	08HN-18C	08HN-18D	08HN-19A	08HN-19B	08HN-19C	08HN-19D	08HN-20A	08HN-20B	08HN-21A	08HN-21B	08HN-21C	08HN-21D
Rock Type	QT	QT	QT	AB	AB	AB	AB	OT	OT	OT	OT	OT	QT
Major elements (wt. %)													
SiO_2	52.80	52.90	52.80	48.10	48.10	48.40	48.40	51.00	51.10	52.10	51.90	52.20	52.20
TiO_2	1.59	1.61	1.62	3.19	3.15	3.16	3.19	2.41	2.43	1.92	1.85	1.95	1.96
$A1_2O_3$	14.30	14.20	14.30	13.10	13.00	13.00	13.30	13.60	13.60	14.30	14.20	14.20	14.20
TFe_2O_3	12.40	12.50	12.40	12.90	12.80	12.80	12.80	12.20	12.20	11.80	12.00	12.00	12.00
MnO	0.13	0.13	0.13	0.16	0.14	0.14	0.16	0.13	0.12	0.13	0.13	0.13	0.13
MgO	6.71	6.62	6.66	8.22	8.22	8.04	7.82	7.46	7.37	6.90	7.05	6.61	6.67
CaO	8.47	8.40	8.46	8.60	8.63	8.68	8.52	8.13	8.06	8.11	8.08	8.02	8.02
Na_2O	2.95	2.95	2.96	3.19	3.34	3.27	3.30	3.37	3.31	3.27	3.30	3.34	3.32
K_2O	0.52	0.56	0.51	1.91	1.89	1.89	1.95	1.35	1.36	1.22	1.18	1.22	1.17
P_2O_5	0.17	0.17	0.17	0.66	0.65	0.65	0.68	0.41	0.41	0.32	0.31	0.33	0.33
Total	100.04	100.04	100.02	100.03	99.92	100.03	100.11	100.06	99.96	100.06	100.00	100.00	100.01
L.O.I.	0.36	0.33	0.41	-0.39	-0.51	-0.41	-0.41	-0.40	-0.22	-0.30	-0.54	-0.26	-0.26
Mg#	54.4	53.9	54.2	58.4	58.5	58.1	57.4	57.4	57.1	56.3	56.5	54.8	55.1
Trace elements (ppm)													
Sc	21.5			19.5		19.1		18.7		18.6	18.5		
V	134			194		177		159		152	140		
Cr	181			229		220		217		197	197		
Co	44.7			49.3		47.6		44.5		46.0	43.9		
Ni	134			144		138		141		162	156		
Cu	76.4			62.9		57.0		62.0		53.0	50.7		
Zn	116			147		139		124		127	117		
Rb	7.4			31.9		30.8		16.9		20.2	19.2		
Sr	286			665		626		486		458	434		
Y	14.8			26.8		28.5		26.2		18.1	17.8		
Zr	92			257		243		172		141	138		
Nb	12.1			48.0		46.2		28.7		25.7	24.6		
Ba	111			636		616		220		215	208		
La	8.5			33.3		33.7		18.3		16.5	16.3		
Ce	18.7			69.0		67.3		37.3		34.4	33.5		
Pr	2.49			8.96		8.84		4.97		4.44	4.27		
Nd	11.2			38.1		37.3		22.1		19.0	18.1		
Sm	3.26			8.82		8.57		5.76		4.84	4.58		
Eu	1.26			2.80		2.85		2.12		1.68	1.72		
Gd	3.69			8.36		8.56		6.09		4.9	4.76		
Tb	0.60			1.22		1.24		0.94		0.75	0.72		
Dy	3.30			6.01		6.10		4.83		3.98	3.78		
Ho	0.61			1.05		1.02		0.84		0.69	0.66		
Er	1.55			2.32		2.40		2.01		1.70	1.62		
Tm	0.21			0.28		0.29		0.25		0.23	0.22		
Yb	1.18			1.62		1.60		1.32		1.31	1.23		
Lu	0.17			0.22		0.23		0.19		0.19	0.17		
Hf	2.53			6.08		5.62		4.12		3.42	3.33		
Ta	0.78			3.14		2.98		1.76		1.56	1.49		
Pb	3.52			2.08		2.18		1.00		2.66	1.76		
Th	1.25			4.59		4.34		2.28		2.61	2.42		
U	0.26			1.04		0.97		0.62		0.69	0.64		
$[La/Sm]_N$	1.69			2.44		2.54		2.05		2.20	2.30		
$[Nb/Th]_N$	1.14			1.23		1.25		1.48		1.16	1.20		
$[Ta/U]_N$	1.54			1.55		1.57		1.46		1.16	1.20		
Sr/Sr*	1.57			1.04		1.00		1.34		1.44	1.43		
Nb/U	46.72			46.15		47.43		46.52		37.41	38.74		
Zr/Hf	36.17			42.27		43.24		41.75		41.23	41.44		
Pb/Ce	0.19			0.03		0.03		0.03		0.08	0.05		

Supplementary Table 3 Continued

Locality	Hainan Island (Wang et al., 2011)												
Sample	08HN-21E	08HN-22A	08HN-22B	08HN-22C	08HN-22D	08HN-23A	08HN-23B	08HN-24A	08HN-24B	08HN-24C	08HN-24D	08HN-25A	08HN-25B
Rock Type	QT	OT	AB	AB	AB	AB	OT	AB	AB	OT	AB	OT	OT
Major elements (wt. %)													
SiO_2	53.10	49.30	49.30	49.50	46.60	49.40	49.20	48.00	47.80	50.60	48.00	49.80	50.00
TiO_2	2.10	2.51	2.50	2.58	2.64	2.60	2.55	2.43	2.41	2.05	2.33	2.10	2.11
$A1_2O_3$	14.10	13.40	13.30	13.50	12.90	13.50	13.30	13.00	13.10	14.20	13.20	13.70	13.80
TFe_2O_3	11.50	12.00	11.90	11.80	13.20	12.00	12.00	12.30	12.60	12.00	12.30	12.40	12.60
MnO	0.12	0.14	0.14	0.13	0.16	0.14	0.14	0.14	0.15	0.13	0.15	0.15	0.14
MgO	5.92	8.28	8.25	7.52	9.25	7.80	8.31	9.55	9.78	7.85	9.80	8.18	8.12
CaO	8.13	9.03	9.05	9.15	9.85	8.99	9.05	9.50	9.37	8.57	9.47	8.92	8.61
Na_2O	3.42	3.01	3.15	3.27	3.05	3.18	2.94	2.98	2.85	2.86	2.73	3.00	3.05
K_2O	1.23	1.92	1.91	1.99	1.67	1.92	1.96	1.59	1.55	1.26	1.51	1.43	1.28
P_2O_5	0.36	0.49	0.49	0.51	0.63	0.52	0.51	0.47	0.44	0.36	0.44	0.35	0.36
Total	99.98	100.08	99.99	99.95	99.95	100.05	99.96	99.97	100.05	99.88	99.93	100.03	100.06
L.O.I.	0.65	-0.39	-0.56	-0.61	-0.62	-0.52	-0.18	-0.62	-0.39	0.12	-0.16	-0.21	-0.16
Mg#	53.1	60.4	60.5	58.3	60.6	59.0	60.4	63.0	63.1	59.0	63.7	59.2	58.7
Trace elements (ppm)													
Sc	15.6	19.7			24.5		20.0	25.6	25.5		25.2	18.0	
V	147	200			238		188	218	208		207	156	
Cr	304	277			222		258	248	259		283	228	
Co	43.4	46.2			50.3		44.8	51.2	50.9		50.4	44.3	
Ni	177	151			172		150	205	205		208	164	
Cu	64.3	47.0			59.1		55.0	60.5	59.9		56.6	49.1	
Zn	141	122			132		115	117	119		112	108	
Rb	40.6	34.2			31.9		33.7	28.5	27.6		25.8	19.5	
Sr	720	617			699		624	573	577		585	453	
Y	17.0	22.3			25.3		22.4	22.2	21.2		20.9	18.5	
Zr	293	213			256		212	205	186		179	143	
Nb	58.0	41.9			63.4		43.6	46.5	44.2		42.2	25.8	
Ba	583	492			505		502	426	407		404	217	
La	36.3	30.8			47.2		31.5	33.5	28.9		28.4	16.8	
Ce	71.5	62.3			96.5		64.0	69.2	60.7		58.0	35.9	
Pr	8.62	7.76			11.5		7.82	8.48	7.48		7.08	4.54	
Nd	33.3	30.8			43.3		31.7	32.8	29.4		28.0	19.4	
Sm	7.26	6.76			8.10		6.90	6.72	6.03		5.97	4.61	
Eu	2.42	2.22			2.54		2.19	2.04	1.95		1.93	1.58	
Gd	6.45	6.53			7.35		6.31	5.97	5.69		5.46	4.75	
Tb	0.91	0.96			1.03		0.94	0.85	0.84		0.82	0.74	
Dy	4.28	4.80			5.24		4.81	4.52	4.46		4.22	3.89	
Ho	0.66	0.83			0.94		0.83	0.81	0.78		0.77	0.71	
Er	1.46	2.04			2.23		1.94	1.98	1.91		1.90	1.66	
Tm	0.18	0.26			0.30		0.24	0.27	0.25		0.25	0.22	
Yb	1.01	1.47			1.80		1.44	1.57	1.53		1.52	1.25	
Lu	0.13	0.20			0.25		0.21	0.23	0.22		0.22	0.18	
Hf	6.47	4.81			5.76		4.88	4.67	4.29		4.10	3.27	
Ta	3.74	2.51			3.93		2.65	2.77	2.73		2.44	1.49	
Pb	2.72	2.96			4.15		3.55	2.84	2.54		2.21	1.54	
Th	5.28	4.61			5.81		4.65	4.31	3.96		3.67	2.31	
U	1.27	0.97			1.38		1.04	1.01	0.95		0.92	0.55	
$[La/Sm]_N$	3.23	2.94			3.77		2.95	3.22	3.10		3.07	2.36	
$[Nb/Th]_N$	1.29	1.07			1.28		1.10	1.27	1.31		1.35	1.31	
$[Ta/U]_N$	1.51	1.33			1.46		1.31	1.40	1.47		1.36	1.39	
Sr/Sr*	1.22	1.15			0.90		1.14	0.99	1.12		1.20	1.40	
Nb/U	45.67	43.42			45.94		41.92	46.04	46.33		46.07	46.99	
Zr/Hf	45.29	44.28			44.44		43.44	43.90	43.36		43.66	43.73	
Pb/Ce	0.04	0.05			0.04		0.06	0.04	0.04		0.04	0.04	

Supplementary Table 3 Continued

Locality	Hainan Island (Wang et al., 2011)												
Sample	08HN-25C	08HN-26A	08HN-26B	08HN-26C	08HN-26D	ZK03-18.1	ZK03-20.1	ZK03-24.4	ZK03-25	ZK03-27	ZK03-27.5	ZK03-29.1	ZK03-30
Rock Type	OT	OT	OT	OT	OT	QT	QT	BS	BS	BS	AB	AB	OT
Major elements (wt. %)													
SiO_2	50.30	51.20	51.20	51.40	51.40	52.40	52.40	46.10	46.10	46.80	46.70	46.20	46.70
TiO_2	2.06	2.13	2.28	2.15	2.18	1.86	1.95	2.51	2.56	2.72	2.62	2.68	2.75
$A1_2O_3$	13.90	14.10	14.00	14.20	14.10	14.10	13.90	13.20	13.10	13.90	13.40	13.40	13.70
TFe_2O_3	12.50	11.60	11.80	11.50	11.60	12.40	11.70	13.70	13.60	14.70	13.70	13.60	14.80
MnO	0.14	0.13	0.13	0.13	0.13	0.10	0.15	0.19	0.19	0.18	0.22	0.18	0.18
MgO	8.11	7.08	6.81	6.88	6.85	6.68	7.03	7.57	7.91	6.62	7.32	7.38	5.54
CaO	8.52	8.95	8.80	8.93	8.91	8.88	8.70	9.88	10.10	10.30	10.30	10.40	10.50
Na_2O	3.00	3.20	3.25	3.20	3.22	2.81	3.06	3.74	3.27	2.02	2.93	3.02	2.20
K_2O	1.20	1.34	1.37	1.35	1.37	0.51	0.88	2.01	1.93	1.46	1.48	1.83	2.14
P_2O_5	0.35	0.35	0.36	0.35	0.36	0.26	0.29	1.21	1.22	1.30	1.23	1.34	1.39
Total	100.07	100.08	100.00	100.09	100.12	100.00	100.05	100.11	99.98	100.00	99.90	100.03	99.90
L.O.I.	-0.26	-0.42	-0.61	-0.40	-0.51	2.17	1.22	1.29	2.34	2.15	2.88	2.64	2.93
Mg#	58.8	57.4	56.1	56.9	56.6	54.3	57.0	55.0	56.2	49.8	54.0	54.5	45.1
Trace elements (ppm)													
Sc	20.1	21.8		21.5				16.2				16.6	
V	154	193		190				150				152	
Cr	250	252		241				131				114	
Co	43.3	43.5		40.6				42.9				44.0	
Ni	168	107		93				129				115	
Cu	59.1	57.9		52.2				51.8				49.7	
Zn	113	126		112				161				160	
Rb	15.7	22.9		21.9				55.4				35.6	
Sr	461	504		479				1327				1341	
Y	19.3	21.1		20.4				33.2				34.7	
Zr	146	170		165				361				360	
Nb	24.5	26.6		26.9				122.0				118.0	
Ba	223	236		245				858				916	
La	17.0	19.5		19.7				97.2				100.0	
Ce	36.3	42.1		41.3				175.0				180.0	
Pr	4.67	5.38		5.34				19.7				20.5	
Nd	19.6	21.9		22.3				72.2				77.1	
Sm	4.82	5.34		5.44				13.00				14.10	
Eu	1.66	1.82		1.91				4.12				4.48	
Gd	4.64	5.26		5.45				11.9				12.3	
Tb	0.71	0.80		0.83				1.54				1.52	
Dy	3.93	4.27		4.32				7.66				7.63	
Ho	0.70	0.76		0.74				1.29				1.28	
Er	1.73	1.94		1.83				3.09				3.03	
Tm	0.22	0.25		0.23				0.39				0.38	
Yb	1.29	1.46		1.37				2.24				2.27	
Lu	0.19	0.20		0.20				0.31				0.31	
Hf	3.38	3.89		3.87				8.55				8.48	
Ta	1.46	1.58		1.67				12.30				12.00	
Pb	1.67	2.14		2.60				5.73				5.58	
Th	2.32	2.82		2.89				13.40				12.90	
U	0.48	0.66		0.69				2.53				3.01	
$[La/Sm]_N$	2.28	2.36		2.34				4.83				4.58	
$[Nb/Th]_N$	1.24	1.11		1.09				1.07				1.08	
$[Ta/U]_N$	1.57	1.23		1.24				2.49				2.04	
Sr/Sr*	1.39	1.34		1.27				1.01				0.97	
Nb/U	51.47	40.30		39.04				48.22				39.20	
Zr/Hf	43.20	43.70		42.64				42.22				42.45	
Pb/Ce	0.05	0.05		0.06				0.03				0.03	

Supplementary Table 3 Continued

Locality	Hainan Island (Wang et al., 2011)											
Sample	ZK03-31	ZK04-10.5	ZK04-26.8	ZK04-30.7	ZK04-9.2	ZK05-20.1	ZK05-22.3	ZK05-25.4	ZK05-28.1	ZK05-32.1	ZK05-33.6	ZK05-36.5
Rock Type	BS	QT	QT	QT	QT	QT	QT	QT	QT	QT	OT	QT
Major elements (wt. %)												
SiO_2	45.90	52.80	52.90	54.20	52.70	51.80	52.00	51.60	51.60	50.90	49.40	47.50
TiO_2	2.66	1.93	1.91	2.73	1.88	1.81	1.97	1.92	1.89	1.96	1.99	2.14
$A1_2O_3$	13.10	13.90	14.30	19.80	13.90	14.10	14.00	13.80	14.10	14.40	14.60	15.40
TFe_2O_3	14.10	12.10	11.40	8.63	11.80	11.80	11.80	12.10	11.60	12.30	13.70	14.10
MnO	0.27	0.16	0.19	0.13	0.14	0.12	0.12	0.13	0.13	0.13	0.13	0.36
MgO	7.00	5.97	4.83	1.86	6.53	7.77	7.13	8.09	8.07	8.07	8.56	7.40
CaO	10.10	9.05	11.50	8.29	8.97	9.06	9.01	8.95	9.18	8.75	8.41	10.34
Na_2O	3.46	3.14	2.96	3.50	3.09	2.81	2.98	2.73	2.76	2.74	2.54	2.24
K_2O	2.16	0.77	0.83	0.39	0.73	0.43	0.62	0.40	0.31	0.45	0.42	0.30
P_2O_5	1.32	0.25	0.26	0.47	0.24	0.28	0.30	0.31	0.31	0.31	0.29	0.36
Total	100.07	100.06	101.08	100.00	99.97	99.98	99.93	100.02	99.96	100.01	100.04	100.15
L.O.I.	4.68	2.43	4.21	3.66	1.63	1.52	1.57	1.05	1.95	2.59	2.79	8.64
Mg#	52.3	52.1	50.6	32.2	54.8	59.2	57.0	59.6	60.4	59.0	57.8	53.7
Trace elements (ppm)												
Sc			21.1			21.6		20.7				23.5
V			138			143		144				154
Cr			214			226		199				282
Co			37.7			44.0		41.4				47.0
Ni			90			173		160				174
Cu			67.7			61.7		65.4				69.0
Zn			120			108		110				134
Rb			16.5			3.2		5.3				4.8
Sr			439			372		397				349
Y			19.5			18.0		19.1				20.0
Zr			117			110		121				123
Nb			20.2			21.5		25.4				25.5
Ba			224			202		182				194
La			16.6			16.0		18.5				19.0
Ce			31.9			31.4		35.8				37.0
Pr			3.98			3.83		4.39				4.61
Nd			16.8			16.1		18.1				18.9
Sm			4.52			4.05		4.48				4.53
Eu			1.63			1.55		1.62				1.64
Gd			4.92			4.58		4.81				4.98
Tb			0.76			0.72		0.75				0.78
Dy			4.20			3.94		4.34				4.32
Ho			0.77			0.73		0.75				0.79
Er			1.89			1.84		1.87				1.93
Tm			0.24			0.23		0.24				0.26
Yb			1.54			1.46		1.49				1.57
Lu			0.22			0.21		0.21				0.23
Hf			3.39			3.18		3.37				3.52
Ta			1.21			1.25		1.45				1.54
Pb			1.89			1.64		2.01				2.60
Th			2.56			2.46		2.80				2.77
U			0.54			0.53		0.58				0.46
$[La/Sm]_N$			2.37			2.55		2.67				2.71
$[Nb/Th]_N$			0.93			1.03		1.07				1.08
$[Ta/U]_N$			1.15			1.21		1.28				1.71
Sr/Sr*			1.55			1.37		1.29				1.08
Nb/U			37.34			40.64		43.72				55.31
Zr/Hf			34.51			34.59		35.91				34.94
Pb/Ce			0.06			0.05		0.06				0.07

Reference

Blichert-Toft, J., Chauvel, C., Albarède, F. (1997) Separation of Hf and Lu for high-precision isotope analysis of rock samples by magnetic sector-multiple collector ICP-MS. *Contrib. Mineral. Petrol.* **127**, 248-260.

Bouvier, A., Vervoort, J.D., Patchett, P.J. (2008) The Lu–Hf and Sm–Nd isotopic composition of CHUR: Constraints from unequilibrated chondrites and implications for the bulk composition of terrestrial planets. *Earth Planet. Sci. Lett.* **273**, 48-57.

Flower M. F., Zhang M., Chen C., Tu K. and Xie G. (1992) Magmatism in the south China basin: 2. Post-spreading Quaternary basalts from Hainan Island, south China. *Chem. Geol.* **97**(1), 65-87.

Ho K., Chen J. and Juang W. (2000) Geochronology and geochemistry of late Cenozoic basalts from the Leiqiong area, southern China. *J. Earth Sci.* **18**(3), 307-324.

Tu K., Flower M. F., Carlson R. W., Zhang M. and Xie G. (1991) Sr, Nd, and Pb isotopic compositions of Hainan basalts (south China): implications for a subcontinental lithosphere Dupal source. *Geology* **19**, 567-569.

Wang X., Li Z., Li X., Li J., Liu Y., Long W., Zhou J. and Wang F. (2011) Temperature, pressure, and composition of the mantle source region of Late Cenozoic basalts in Hainan Island, SE Asia: a consequence of a young thermal mantle plume close to subduction zones? *J. Petrol.* **53**, 177-233.

Zou H. and Fan Q. (2010) U–Th isotopes in Hainan basalts: Implications for sub-asthenospheric origin of EM2 mantle endmember and the dynamics of melting

beneath Hainan Island. *Lithos* **116**(1), 145-152.